Switched Dynamic Event-Triggered Control for String Stability of Nonhomogeneous Vehicle Platoons with Uncertainty Compensation

Rafael Silva, Anh-Tu Nguyen, Thierry-Marie Guerra, Fernando Souza, Luciano Frezzatto

Switched Dynamic Event-Triggered Control for String Stability of Nonhomogeneous Vehicle Platoons with Uncertainty Compensation

Rafael Silva, Anh-Tu Nguyen*, *Senior Member, IEEE*, Thierry-Marie Guerra, Fernando Souza, Luciano Frezzatto

***Abstract*—This paper investigates cooperative adaptive cruise control (CACC) for intelligent and connected vehicles using a predecessor-follower (PF) topology under event-triggered communication and modeling uncertainties. These uncertainties in the vehicular platoon can challenge the well-known homogeneity and linearity assumptions of the CACC. To address this issue, we propose a disturbance observer (DOB) to estimate both the parametric uncertainty and the unmeasured external signals. The DOB-based disturbance estimate is directly incorporated into the feedback linearization control law for uncertainty compensation. To assess the individual stability of each vehicle and the string stability of the nonhomogeneous platoon, we formulate overlapping dynamics that model the interconnection of only those vehicles directly exchanging information. This formulation of overlapping dynamics also facilitates the scalability of the platoon, i.e., we can conveniently increase the number of vehicles in the platoon without compromising the complexity of the stability analysis. Using a suitable Lyapunov-Krasovskii functional and the null-term relaxation technique, we derive sufficient conditions to design a switched dynamic event-triggered controller (ETC) that ensures both individual stability and string stability. With the proposed switching ETC approach, the event-triggering condition is only evaluated after a predefined constant period, ensuring a lower bound between events to avoid Zeno behavior. Extended from the $\mathcal{L}_2$ stability concept to explicitly account for the uncertainty effects of the nonhomogeneous platoon, the ETC design conditions are formulated as a convex optimization problem under linear matrix inequalities to maximize the inter-event time. The effectiveness of the proposed ETC approach is validated through extensive simulations and comparisons using an uncertain CACC setup.**

***Index Terms*—Cooperative adaptive cruise control, intelligent and connected vehicles, vehicle platooning system, string stability, event-triggered control, disturbance observer.**

This work was supported by the French Ministry of Higher Education and Research, by the CNRS, by the Hauts-de-France region, by the Coordination for the Improvement of Higher Education Personnel - Brazil (CAPES) through the Academic Excellence Program, by the project InSAC (National Institute of Science and Technology for Cooperative Autonomous Systems Applied to Security and Environment) under the grants CNPq (Conselho Nacional de Desenvolvimento Científico e Tecnológico) 465755/2014-3 and 88887.513093/2020-00, Fundação de Amparo à Pesquisa do Estado de Minas Gerais (FAPEMIG), and São Paulo Research Foundation (FAPESP) 2014/50851-0, and also by the grants CNPq: 312034/2020-2, FAPEMIG: APQ-00543-217 and APQ-00630-23, and Universidade Federal de Minas Gerais.

R. Silva, A.-T. Nguyen and T.-M. Guerra are with the LAMIH Research Center, UMR CNRS 8201, Université Polytechnique Hauts-de-France, Valenciennes, France. R. Silva is also with the Universidade Federal de Minas Gerais, Belo Horizonte, Brazil. A.-T. Nguyen is also with the INSA Hauts-de-France, Valenciennes, France (e-mail: {rafael.silva,tnguyen,guerra}@uphf.fr).

F. Souza and L. Frezzatto are with the Universidade Federal de Minas Gerais, Belo Horizonte, Brazil (e-mail: {fosouza,lfrezzatto}@ufmg.br).

*Corresponding author: Anh-Tu Nguyen (nguyen.trananhtu@gmail.com).

I. Introduction

Traffic congestion and accidents have constantly increased with a larger population, resulting in problems such as transportation delays, traffic jams, and increased fuel consumption [1]–[3]. In this context, high-level platoon coordination [4], [5] together with physical-level platooning control [6]–[8] have been considered a promising solution. Through platooning, vehicles can travel in a string-like configuration, maintaining controlled distance and velocity according to a predefined strategy/policy and safety constraints [9], [10]. With automatic distance control, vehicles can maintain shorter and regular distances without compromising safety, thereby reducing traffic jams and optimizing transportation.

Adaptive cruise control (ACC) is a well-known concept for vehicle management, involving a leader (designated here with index 0) and N follower vehicles in a string, with a distance policy that can be fixed [11]–[13] or time-based [14], [15]. The fixed distance policy can provide a closer vehicular distance but is inefficient for vehicles traveling at higher speeds [9]. In such cases, time-headway policies are more versatile, as the distance is controlled based on the standstill distance along with the speed of the vehicles [9], [16]. As an extension of ACC, cooperative adaptive cruise control (CACC) further improves platooning control results by combining sensor measurements with information exchanged between vehicles [17], [18]. Depending on the communication between the vehicles of the platoon and how the information flows, various flow topologies can be distinguished. The predecessor-leader-follower (PLF) and its variants consider the sharing of information from a leader vehicle among all vehicles in the network, which can be either unidirectional or bidirectional [19], [20]. The predecessor-follower (PF) topology closely resembles human driving behavior [9], [14], [15]. In this case, information flows from the ith vehicle after the leader to the $(i+1)$th vehicle, i.e., the follower of the ith vehicle. Hence, only the first vehicle (vehicle 1) receives information from the leader (vehicle 0). Although the PF topology is the simplest in terms of the number of sensors and communication devices, it poses additional challenges to ensure string stability [9], [21]. String stability, an important and desired property, ensures that disturbances are not amplified throughout the string of platooning vehicles. This reduction in disturbances can lead to a decrease in excessive braking, thereby contributing to the alleviation of traffic problems [11], [15], [22].

To ensure string stability, various approaches have been

proposed in the literature based on frequency-domain analysis (in terms of $\mathcal{H}_\infty$ norm) such as [23]–[25], and time-domain methods (in terms of $\mathcal{L}_p$ norms) as demonstrated in [14], [15], [22]. The time-domain approach relies on evaluating the $\mathcal{L}_p$ norm between the leader input or perturbations and the output of the last vehicle in the platoon. This can also be studied by evaluating the $\mathcal{L}_p$ norm between the input and the output of the subsystem that composes the string, a concept sometimes referred to as weak string stability [14], [15].

A. Modeling Uncertainties of Vehicular Platooning Systems

In most works on CACC, a common assumption is the homogeneity and linearity of the platoon [14], [15], [19], [21]–[23], [26]. Although this assumption can be achieved through feedback linearization techniques, the procedure requires precise knowledge of the vehicle parameters. Parametric uncertainties and unmeasured external variables can cause mismatches, resulting in nonhomogeneous platooning systems [27]–[30]. To overcome these problems, Wang et al. [31] propose an intermediate-based robust observer to jointly estimate the sensor and actuator faults as well as matched disturbances, whose effects can be compensated via a robust non-fragile fault-tolerant control method. In [32], a proportional multiple-integral observer is employed to simultaneously estimate the state and a lumped disturbance, which is compensated via a tube-based model predictive control scheme. However, the issue of string stability for vehicle platoons is not addressed in [31], [32]. Alternatively, the authors in [28] consider a filtering technique to attenuate the effects of disturbances, while the works [27], [29] explore Lyapunov-like string stability conditions with disturbances. These works evaluate string stability based on the overall platoon dynamics describing the relationship between the input of the leader and the output of the last vehicle. Note that the need to consider the overall platoon dynamics can significantly increase the stability analysis complexity. Indeed, in this case, whenever new vehicles are added to the platoon, the stability analysis conditions must be reevaluated. Moreover, as the number of vehicles in the platoon grows, more decision variables and constraints are involved in the optimization-based stability analysis, potentially yielding more conservative results or even infeasible solutions. These factors compromise the scalability of the application of such stability conditions. In contrast, we propose here to address the uncertainty issue in platooning control through feedback linearization combined with a disturbance compensation technique. To this end, mismatches caused by parametric uncertainties and exogenous disturbance effects are modeled as a single *virtual* disturbance signal, which is estimated and compensated by a disturbance observer (DOB) with a simple structure. The DOB-based disturbance estimate is directly integrated into the feedback control law. Consequently, the platooning system dynamics are only influenced by the disturbance estimation error, representing the difference between modeling uncertainties and their estimated counterparts. To address the impact of the disturbance estimation error, we propose an extension of the $\mathcal{L}_2$ norm stability conditions to assess string stability. Specifically, classical string stability can be ensured in the presence of significant uncertainties through an effective disturbance compensation.

B. Wireless Communication and Event-Triggered Control

In addition to traffic problems and fuel consumption associated with the stability of each individual vehicle and string stability of the platoon, communication between vehicles plays a crucial role in CACC [12], [33], [34]. In early studies, platoons with vehicle-to-vehicle (V2V) communication adopted continuous or periodic communication among vehicles [9], [35], [36]. It is clear that these communication schemes impose a large bandwidth and energy consumption, as information is transmitted regardless of any network condition. For this reason, event-triggered controllers (ETC) appear as an appropriate strategy to reduce the burden of excessive network use [37]. For an ETC scheme, information is only transmitted based on an event-triggering mechanism (ETM), which evaluates the next communication instant based on the current and last transmitted information.

Some ETC applications in CACC include cases with static event-triggering mechanisms, whose parameters are time-independent [19], [38]–[40]. However, due to the static nature of the triggering mechanisms, these ETC schemes can be conservative and may result in more transmissions than necessary. To enhance the performance of static ETMs, dynamic ETMs can be applied, where the involved parameters vary over time [12], [14], [41] In addition, the triggering conditions of dynamic ETMs can change according to the information to be transmitted. One of the primary challenges in event-triggered communications is preventing Zeno behavior. This undesirable phenomenon occurs when an infinite number of transmissions (or events) take place within a finite time interval, i.e., the time between events converges to zero. It is important to note that in scenarios without exogenous disturbances and with full transmission of system states, a positive minimum time between consecutive events can be readily imposed in ETMs to prevent Zeno behavior [14], [37], [42]. However, in cases involving partial transmission of states and/or perturbed systems, significant technical effort is required to ensure Zeno-free behavior [43]. Therefore, when parametric uncertainties and exogenous disturbances are explicitly considered in the design of platooning ETC, the standard ETMs in [14], [37], [42] can no longer guarantee a positive lower bound for the inter-event time (IET) to prevent Zeno behavior. To ensure a minimum time between consecutive transmissions, as in [44], we impose an enforced waiting period, ensuring that a new transmission does not occur before this time has elapsed, regardless of the event-triggering condition. To account for the imposed minimum time, we model the platooning dynamics as a switching system based on the time intervals during which the event-triggering conditions are considered or not. Using this switching modeling formulation, we propose a relevant switched dynamic event-triggering condition to maximize the IET, thereby reducing the communication workload.

C. Main Proposition and Contributions

We consider a vehicular platoon with one leader and N followers, as depicted in Fig. 1. The leader vehicle has the

index $i = 0$, and is denoted by Σ_0, while the other vehicles have indices $i = 1, \ldots, N$, and are denoted by Σ_i. For this platoon setup, in addition to the measurements provided by sensors, vehicles also share information through a network, with transmission flowing only from vehicle Σ_{i-1} to vehicle Σ_i. The problem of interest is to ensure the individual stability of vehicle Σ_i and string stability, i.e., input-to-output stability from Σ_0 to Σ_N, while minimizing the required communication between vehicles. In particular, we focus on the scenario where the vehicle parameters are not precisely known, i.e., a nonhomogeneous platoon. To this end, we propose a dynamic event-triggering control method for the string stability of uncertain vehicle platoons. To address parametric uncertainty, we model its influences and unmeasured external signals as a virtual additive disturbance affecting the nominal platooning system. Using a DOB, this virtual disturbance is estimated and incorporated into the feedback control law for compensation purposes. To minimize communication between vehicles in the nonhomogeneous platoon, we propose a dynamic event-triggering condition with an enforced minimum time between consecutive transmissions. To assess the individual stability of each vehicle and string stability, we formulate an overlapping dynamics $\Sigma_{i,i-1}$ that models the interconnection of vehicles exchanging information, i.e., Σ_i and Σ_{i-1}, for $i = 1, \ldots, N$. Additionally, inspired by [44], a switching modeling approach is employed to consider the ETC mechanism.

Under event-triggered communication and the proposed DOB-based uncertainty compensation, we extend the classical $\mathcal{L}_2$ stability to ensure string stability of the nonhomogeneous platoon in the presence of the disturbance estimation error. In contrast to [13], the stability conditions are evaluated for a single overlapping system $\Sigma_{i,i-1}$, rather than the interconnection of all vehicles, i.e., $\Sigma_{0,N}$. Moreover, in contrast to [14], [15], the proposed $\mathcal{L}_2$ stability conditions explicitly account for the uncertainties of the platooning system. Using a suitable Lyapunov-Krasovskii functional (LKF) [45] and the null-term relaxation technique [46], we propose an emulation approach to design the ETC mechanism, ensuring the $\mathcal{L}_2$ stability of the platooning system while maximizing the inter-event time. The ETC design is reformulated as an optimization problem under linear matrix inequality (LMI) constraints, which can be conveniently and effectively solved using common numerical solvers [47]. Specifically, the main contribution of the paper can be summarized as follows.

- A DOB-based disturbance compensation scheme is proposed for feedback linearization control of nonhomogeneous platoons. The effects of disturbance estimation errors can explicitly be accounted for in the string stability analysis under event-triggered communication using an extended $\mathcal{L}_2$ stability framework.
- A switched dynamic ETM is proposed with relaxed LKF-based design conditions to ensure $\mathcal{L}_2$ string stability of the nonhomogeneous platoon while minimizing the number of transmissions and avoiding Zeno behavior.
- The ETC design, based on a simple overlapping system instead of the interconnection of all vehicles, enables the *scalability* of string stability conditions.

Moreover, a comprehensive comparative study is conducted with various ETC schemes in recent literature to emphasize the effectiveness of the proposed platooning control method.

Notation. $\mathbb{R}^n$ denotes the n-dimensional Euclidean space, $\mathbb{R}^{n\times m}$ is the set of $n\times m$ matrices with real entries. For vectors $x \in \mathbb{R}^n$ and $y \in \mathbb{R}^m$, $\|x\|$ stands for the vector Euclidean norm of x, and $\mathrm{col}(x, y)$ is the same as $[x^T \ y^T]^T$. For a matrix X, X^T denotes its transpose, X^{-1} its inverse, $\mathrm{Tr}(X)$ denotes its trace, and $\mathrm{He}(X) = X^T + X$. For a symmetric matrix P, $P \succ 0$ stands for a positive definite. The symbol $*$ in a matrix denotes a symmetric component. For matrices $Y_1, Y_2, \ldots, Y_p$, $\mathrm{diag}(Y_1, Y_2, \ldots, Y_p)$ stands for block diagonal matrix with entries Y_i. The $\mathcal{L}_2$ norm of a time-dependent vector $x(t)$ is denoted by $\|x\|_{\mathcal{L}_2} = \sqrt{\int_0^\infty \|x(t)\|^2 dt}$. We use the subscript n to indicate known (nominal) values. For example, M_i and $M_{i,n}$ respectively represent the unknown and nominal values of parameter M_i. Moreover, for a function $f(\cdot)$ that depends on a set of parameters, we denote $f_n(\cdot)$ to indicate that the expression is computed using the nominal values of the involved parameters.

II. Modeling and Preliminaries

This section first describes the platooning control framework under consideration. Then, we present the related vehicle dynamics and the respective distance policy.

A. Platooning Control Framework

Considering the vehicular platoon shown in Fig. 1, the main goal is to maintain a safe distance between all vehicles. This distance policy is composed of a fixed distance for the vehicles in standby and a time-based gap that depends on the vehicle velocity. The homogeneity assumption is commonly employed in vehicular platoons to simplify control design and stability analysis, especially when the feedback linearization control technique is used [14], [22], [39]. However, this assumption is not realistic in practice. Even considering the feedback linearization procedure, mismatches caused by modeling uncertainties lead to nonhomogeneous platoons. To align more closely with real-world scenarios, we assume that only nominal (approximate) values of vehicle parameters, obtained through identification, measurements, or provided by manufacturers, are available for platooning control design. Additionally, we consider the effect of the unknown rolling resistance coefficient, treated as an exogenous disturbance. For control design, we remodel the uncertain nonhomogeneous platooning system by incorporating parametric uncertainties and unmeasured exogenous disturbances into a *virtual* disturbance. Subsequently, we introduce a DOB-based estimate of this disturbance into the feedback linearizing control law to compensate for uncertainty effects and enhance controller robustness.

For the CACC approach, to achieve the desired distance policy, the vehicles exchange information among themselves. In this paper, we consider the PF flow topology [21], as shown in Fig. 1, with vehicle 0 as the leader and vehicle i as the ith follower, where information flows only from vehicle Σ_{i-1} to vehicle Σ_i. Having information shared only between

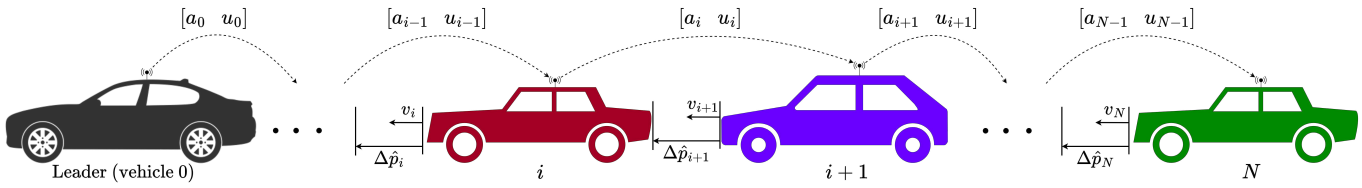

Fig. 1: Platooning PF topology with one leader (vehicle 0) and N following vehicles. v_i and $\Delta\hat{p}_i$ denote the velocity and the relative distance between vehicles, while the transmitted signals a_i and u_i denote acceleration and desired acceleration input.

near vehicles reduces requirements in communication, as long-range communication is more power-consuming and leads to more delays [9]. However, not having information from the leader shared with all the vehicles increases the difficulty in ensuring string stability [9].

To ensure both platooning string stability and individual vehicle stability under event-triggering communication, we first define an overlapping dynamics $\Sigma_{i,i-1}$ by combining the dynamics Σ_i with a part of the dynamics of Σ_{i-1}. The string stability is ensured by evaluating the $\mathcal{L}_2$ stability between the input and the output of these overlapping systems $\Sigma_{i,i-1}$. In addition, the overlapping system $\Sigma_{i,i-1}$ also includes the effect of uncertainties, modeled as a virtual disturbance, and its DOB-based compensation. Hence, by evaluating $\mathcal{L}_2$ stability the influence of the disturbance attenuation is also considered. Moreover, the stability condition is evaluated for a single subsystem $\Sigma_{i,i-1}$ instead of the combined dynamics from Σ_0 to Σ_N. This reduces the complexity of the stability analysis, as it is independent of the number of vehicles in the platoon.

The communication is wireless, and, since fixed-time transmissions can lead to redundant transmission and network overflow [37], [44], information is updated according to a decentralized event-triggering mechanism, as shown in Fig. 2. Vehicle i receives the acceleration and the desired acceleration $[a_{i-1} \;\; u_{i-1}]$, as well as the measured information about the position and velocity $[p_{i-1} \;\; v_{i-1}]$ from vehicle $(i-1)$. The control law of vehicle i is composed of both feedforward and feedback components. The feedforward component is computed using $[a_{i-1} \;\; u_{i-1}]$, while the feedback component is computed using $[p_{i-1} \;\; v_{i-1}]$, as well as the internal states $[p_i \;\; v_i \;\; a_i]$ of vehicle i. The control signal is filtered to provide the desired acceleration u_i, which, along with the internal state a_i, is transmitted to vehicle $(i+1)$ according to an event-triggering mechanism. The proposed ETM is decentralized, relying only on the measured signals of the vehicle itself and not on the measurements of other vehicles. To avoid Zeno behavior, the event-triggered control condition is evaluated only after a fixed waiting time, resulting in an enforced minimum time between events. A switching approach is considered to model the system with this imposed minimum IET and the ETC scheme is designed based on this switching model. In particular, to reduce the communication load, we propose a dynamic ETC scheme.

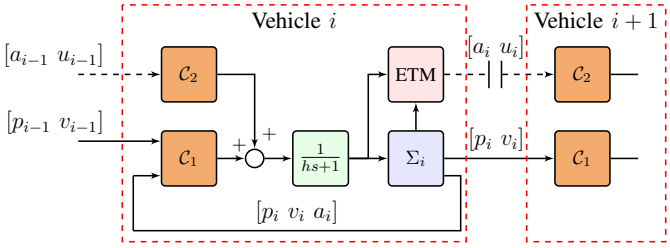

Fig. 2: Communication loop of the proposed event-triggered CACC setup. Σ_i denotes the dynamics of the ith vehicle. $\mathcal{C}_1$ and $\mathcal{C}_2$ respectively represent the feedback and feedforward control laws. $[p_i, v_i]$ denotes the measured state, while $[a_i, u_i]$ denotes the transmitted state.

B. Vehicle Dynamics and Distance Policy

For each vehicle in the platooning system, we consider the following dynamics [48]:

$$\dot{p}_i = v_i \tag{1a}$$

$$\dot{v}_i = \frac{1}{M_i}\left(R_{h,i}T_i - m_i g F_{r,i} - b_i v_i - c_i v_i^2\right) \tag{1b}$$

$$\dot{T}_i = -\frac{1}{\tau_i}T_i + \frac{1}{\tau_i}u_{e,i} \tag{1c}$$

where p_i and v_i are the vehicle position and velocity, T_i is the engine torque, and $u_{e,i}$ is the engine desired torque. The unknown rolling resistance coefficient $F_{r,i}$ is considered as an exogenous disturbance. The auxiliary parameters M_i and $R_{h,i}$ in (1b) are respectively defined as

$$M_i = \frac{(m_i h_{w,i}^2 + J_{r,i} + J_{f,i})R_{g,i}^2 + J_{e,i}}{h_{w,i}^2 R_{g,i}^2} \tag{2}$$

$$R_{h,i} = (h_{w,i}\, R_{g,i})^{-1}. \tag{3}$$

The vehicle parameters are explained in Table I, where the subscript i is used to indicate that these values can change among vehicles. Note that in this paper, we consider that these vehicle parameters cannot be precisely known, leading to parametric uncertainties, and only their nominal values are available for control design.

Let us denote $\dot{v}_i = a_i$, then the acceleration dynamics can be derived from (1b) as

$$\dot{a}_i = \frac{1}{M_i}\left(R_{h,i}\dot{T}_i - (b_i + 2c_i v_i)a_i\right) \tag{4}$$

Substituting $\dot{T}_i$ from (1c) in (4) with T_i in (1b), we obtain

$$\dot{p}_i = v_i \tag{5a}$$

TABLE I: Vehicle model parameters.

Parameters	Description
m_i	Mass of the vehicle (kg)
$R_{g,i}$	Gear ratio (–)
$h_{w,i}$	Height of center of wheel (m)
$J_{e,i}$	Engine/transmission inertia (kg·m^2)
$J_{r,i}$	Rear wheel inertia (kg·m^2)
g	Gravitational acceleration (m/s^2)
$J_{f,i}$	Front wheel inertia (kg·m^2)
b_i, c_i	Resistance force coefficients (kg/s, kg/(m·s))
τ_i	Time constant of the longitudinal dynamics (s)

$$\dot{v}_i = a_i \tag{5b}$$
$$\dot{a}_i = f_i(v_i, a_i) + B_i u_{e,i} + D_i F_{r,i} \tag{5c}$$

with

$$\begin{aligned} f_i(v_i, a_i) &= -\left(\frac{1}{\tau_i} + \Lambda_i\right) a_i - \frac{1}{M_i \tau_i}\left(b_i + c_i v_i\right) v_i \\ \Lambda_i &= \frac{1}{M_i}\left(b_i + 2c_i v_i\right), \quad B_i = \frac{R_{h,i}}{M_i \tau_i}, \quad D_i = \frac{m_i g}{M_i \tau_i}. \end{aligned} \tag{6}$$

Based on the vehicle dynamics (1), let $\Delta\hat{p}_i = p_{i-1} - p_i - L_{c,i}$ be the relative distance between vehicles in the platoon, with $L_{c,i}$ the vehicle length. We define the distance policy error as

$$\Delta p_i = \Delta\hat{p}_{i,i-1} - \Delta p_{d,i}. \tag{7}$$

The time gap distance policy in (7) is given by

$$\Delta p_{d,i} = r_i + h v_i \tag{8}$$

where r_i is the standstill distance for each vehicle, and h is the time gap, which is constant for all vehicles of the platoon.

C. String Stability and $\mathcal{L}_2$ Stability

In this paper, string stability is evaluated based on the $\mathcal{L}_2$ string stability proposed in [22], which is defined as follows.

Definition 1. Let $\bar{x}_i = [\Delta p_i, v_{i-1} - v_i, a_i]$ and $\bar{x}(t) = \mathrm{col}(\bar{x}_1, \ldots, \bar{x}_N)$ be the lumped state of all vehicles. Moreover, let u_0 be an exogenous input, and $z_i = h(\bar{x}_i)$ be a performance output. The vehicular platoon is $\mathcal{L}_2$ string stable if there exist a constant γ_0 and a $\mathcal{K}$-function $\rho(\cdot)$ such that for any initial condition $\bar{x}(0)$, we have

$$\|z_i\|_{\mathcal{L}_2} \leq \gamma_0 \|u_0\|_{\mathcal{L}_2} + \rho(\|\bar{x}(0)\|), \quad i = 1, \ldots, N. \tag{9}$$

In Definition 1, the exogenous input u_0 refers to the leader input, while z_i is a performance output of each vehicle and will be defined later in Section III. This definition of string stability is similar to that in [14], which is a particular case of the general $\mathcal{L}_p$ string stability discussed in [8]. Moreover, condition (9) also shows a clear relationship between this string stability definition and the classical $\mathcal{L}_2$ stability described in [49, Chapter 6.4].

D. Platooning Control Problem Statement

The proposed event-triggered CACC method is based on the feedback linearization technique together with a DOB-based disturbance estimation to deal with a platoon setup with nonhomogeneous vehicles. The designed ETC controller satisfies the following requirements:

- Ensure the individual stability of each vehicle and the string stability of the vehicular platoon, based on $\mathcal{L}_2$ stability conditions.
- Minimize the influence of the disturbance estimation error via $\mathcal{L}_2$ norm.
- Reduce the number of transmissions for the ETC and avoid Zeno behavior.

III. Control Problem Formulation

This section formulates the problems of disturbance compensation and switching system modeling for ETC design.

A. DOB-Based Uncertainty Compensation

The nonlinear model (5) describes the vehicle dynamics subject to parametric uncertainties and an exogenous unmeasured disturbance, as discussed in Section II. Based on (5c), we define the following nominal dynamics without the exogenous disturbance $F_{r,i}$:

$$\dot{a}_{i,n} = f_{i,n}(v_i, a_i) + B_{i,n} u_{e,i}. \tag{10}$$

where $f_{i,n}(v_i, a_i)$ and $B_{i,n}$ are respectively computed using the same expressions of $f_i(v_i, a_i)$ and B_i in (6) with nominal values of vehicle parameters. From the expressions of the uncertain nonhomogeneous platooning system (5c) and its nominal model (10), we define a *virtual* disturbance as

$$d_i = f_{i,n}(v_i, a_i) - f_i(v_i, a_i) + (B_{i,n} - B_i) u_{e,i} - D_i F_{r,i} \tag{11}$$

which represents the mismatch between (5c) and (10). Considering the virtual disturbance (11) and the nominal dynamics (10), we can rewrite (5c) in the form

$$\dot{a}_i = f_{i,n}(v_i, a_i) + B_{i,n} u_{e,i} - d_i. \tag{12}$$

From expression (12), we propose the following disturbance observer for system (5):

$$\begin{aligned} \dot{\zeta}_i &= \frac{\partial L(a_i)}{\partial a_i}\left(f_{i,n}(v_i, a_i) + B_{i,n} u_{e,i} - \hat{d}_i\right) \\ \hat{d}_i &= \zeta_i - L(a_i) \end{aligned} \tag{13}$$

where ζ_i is the internal state of the DOB, $L(a_i)$ is the observer gain, and $\hat{d}_i$ is the estimated disturbance. Let us define the disturbance estimation error as $e_{d,i} = \hat{d}_i - d_i$. Considering that d_i has slow variations, i.e, $\dot{d}_i \approx 0$, the disturbance error dynamics can be defined from (12) and (13) as

$$\dot{e}_{d,i} = -\frac{\partial L(a_i)}{\partial a_i} e_{d,i}. \tag{14}$$

Hence, by choosing $L(a_i)$ such that system (14) is asymptotically stable, it follows that $\hat{d}_i \to d_i$.

Using the disturbance observer (13), we propose the following linearizing control law for system (5):

$$u_{e,i} = \frac{1}{B_{i,n}} \left(-\frac{1}{\tau_d} a_i - f_{n,i}(v_i, a_i) + \frac{1}{\tau_d} u_i + \hat{d}_i \right) \tag{15}$$

where u_i is the desired acceleration input, and τ_d is the desired time constant, which is specified considering an estimation of the real time constant of the vehicle longitudinal dynamics. Applying the control law (15) to the uncertain system (5), with (5c) rewritten as (12), and combining with (7), we obtain the following linearized vehicle dynamics:

$$\Sigma_i : \begin{cases} \Delta \dot{p}_i = v_{i-1} - v_i - h a_i \\ \dot{v}_i = a_i \\ \dot{a}_i = -\frac{1}{\tau_d} a_i + \frac{1}{\tau_d} u_i + e_{d,i} \end{cases} \tag{16}$$

for vehicles $i = 1, \ldots, N$. For the leader vehicle, we have $\Delta p_i = 0$. Then, the leader vehicle dynamics are given by

$$\Sigma_0 : \begin{cases} \dot{v}_0 = a_0 \\ \dot{a}_0 = -\frac{1}{\tau_d} a_0 + \frac{1}{\tau_d} u_0 + e_{d,0} \end{cases} \tag{17}$$

With an effective DOB-based disturbance estimation, i.e., $\|e_{d,i}\| \approx 0$, the systems Σ_i, for $i = 0, \ldots, N$, reduce to the homogeneous case and common known results on homogeneous platoon control can be applied.

Commonly used in both ACC and CACC setups [14], [22], [24], to compensate for the effect of the distance policy with a constant time gap, we introduce the following filter for all vehicles Σ_i, with $i = 0, \ldots, N$:

$$\dot{u}_i = -\frac{1}{h} u_i + \frac{1}{h} \xi_i \tag{18}$$

where ξ_i is the control input signal to be designed.

B. Overlapping System for String Stability Analysis

To evaluate the string stability of the platooning system, first, we form the following overlapping system between vehicles Σ_i and Σ_{i-1} from system (16) and filter (18):

$$\Sigma_{i,i-1} : \begin{cases} \Delta \dot{p}_i = \Delta v_i - h a_i \\ \Delta \dot{v}_i = a_{i-1} - a_i \\ \dot{a}_i = -\frac{1}{\tau_d} a_i + \frac{1}{\tau_d} u_i + e_{d,i} \\ \dot{u}_i = -\frac{1}{h} u_i + \frac{1}{h} \xi_i \\ \dot{a}_{i-1} = -\frac{1}{\tau_d} a_{i-1} + \frac{1}{\tau_d} u_{i-1} + e_{d,i-1} \\ \dot{u}_{i-1} = -\frac{1}{h} u_{i-1} + \frac{1}{h} \xi_{i-1} \end{cases} \tag{19}$$

where $\Delta v_i = v_{i-1} - v_i$ is the difference in velocity. Note that the dynamics of the system $\Sigma_{i,i-1}$ are composed of both the dynamics of vehicle Σ_i and vehicle Σ_{i-1}. Let us denote $x_{1,i} = [\Delta p_i \ \Delta v_i \ a_i \ u_i]^T$ and $x_{2,i-1} = [a_{i-1} \ u_{i-1}]^T$. Then, the following control law is chosen for system (19):

$$\xi_i = \underbrace{K_1 x_{1,i}(t)}_{u_{\text{fb}}(t)} + \underbrace{K_2 x_{2,i-1}(t_k)}_{u_{\text{ff}}(t_k)} \tag{20}$$

with $x_{2,i-1}(t_k) = [a_{i-1}(t_k) \ u_{i-1}(t_k)]^T$, which is transmitted from vehicle $(i-1)$ to vehicle i. Note from (20) that $u_{\text{fb}}(t) = K_1 x_{1,i}(t)$ represents the feedback control component, and $u_{\text{ff}}(t_k) = K_2 x_{2,i-1}(t_k)$ represents the feedforward control component. The feedback and feedforward gains K_1 and K_2 are constant for all vehicles Σ_i, with $i = 1, \ldots, N$. These control gains K_1 and K_2 are chosen to reduce the distance policy error, following the guidelines in Remarks 1 and 2.

Remark 1. The feedback gain K_1 is determined to ensure the *individual* stability of the vehicles. This control gain can be obtained using any control design technique, such as $\mathcal{H}_\infty$ control. However, specifically for a linear homogeneous platoon, as shown in [22], [23], if the gain matrix $K_1 = [K_{11} \ K_{12} \ K_{13} \ K_{14}]$ is chosen such that

$$K_{11} > 0, \quad K_{12} > \tau_d K_{11}, \quad K_{13} = h K_{12}, \quad K_{14} = 0 \tag{21}$$

then each vehicle of the platoon is individually stable. In this work, due to the effectiveness of the proposed DOB-based uncertainty compensation for nonhomogeneous platoons, we can also choose K_1 following (21).

Remark 2. As discussed in [23], the feedforward control $u_{\text{ff}}(t_k) = K_2 x_{2,i-1}(t_k)$ is utilized to effectively counteract the influence of $u_{i-1}(t_k)$ in steady state, i.e., $u_{\text{ff}}(t_k) \to u_{i-1}(t_k)$, in the dynamics of the distance policy error $\text{col}(\Delta \dot{p}_i, \Delta \ddot{p}_i, \Delta \dddot{p}_i)$. Thus, with $x_{2,i-1}(t_k) = [a_{i-1}(t_k) \ u_{i-1}(t_k)]^T$ and $K_2 = [K_{21} \ K_{22}]$, it follows that in steady state, we should have

$$u_{\text{ff}}(t_k) = K_{21} a_{i-1}(t_k) + K_{22} u_{i-1}(t_k) \to u_{i-1}(t_k). \tag{22}$$

Moreover, with effective DOB-based uncertainty compensation, i.e., $e_{d,i} \approx 0$, it follows from (16) that

$$\dot{a}_i = -\frac{1}{\tau_d} a_i + \frac{1}{\tau_d} u_i. \tag{23}$$

We can observe from (23) that the acceleration a_i converges to the desired acceleration u_i in steady state. Therefore, it directly follows from (22) that in steady state, one should have

$$K_{21} + K_{22} = 1. \tag{24}$$

Then, the values of K_{21} and K_{22} can be chosen to fulfill (24).

The overlapping system (19) together with the control law (20) can be further recast in the closed-loop system

$$\Sigma_{i,i-1} : \begin{cases} \dot{x}_{1,i} = (A_1 + B_1 K_1) x_{1,i} + A_2 x_{2,i-1} \\ \qquad\qquad + B_1 K_2 x_{2,i-1}(t_k) + E_1 e_{d,i} \\ \dot{x}_{2,i-1} = A_3 x_{2,i-1} + D_1 \xi_{i-1} + E_2 e_{d,i-1} \end{cases} \tag{25}$$

with

$$A_1 = \begin{bmatrix} 0 & 1 & -h & 0 \\ 0 & 0 & -1 & 0 \\ 0 & 0 & -1/\tau_d & 1/\tau_d \\ 0 & 0 & 0 & -1/h \end{bmatrix}, \quad A_2 = \begin{bmatrix} 0 & 0 \\ 1 & 0 \\ 0 & 0 \\ 0 & 0 \end{bmatrix}$$

$$A_3 = \begin{bmatrix} -1/\tau_d & 1/\tau_d \\ 0 & -1/h \end{bmatrix}, \quad B_1 = \begin{bmatrix} 0 & 0 & 0 & 1/h \end{bmatrix}^T$$

$$D_1 = \begin{bmatrix} 0 & 1/h \end{bmatrix}^T$$

$$E_1 = \begin{bmatrix} 0 & 0 & 1 & 0 \end{bmatrix}^T, \quad E_2 = \begin{bmatrix} 1 & 0 \end{bmatrix}^T.$$

Moreover, for string stability analysis, we define the following performance output to evaluate the $\mathcal{L}_2$ stability:

$$z_i = \xi_i, \quad i = 2, \dots, N \tag{26}$$

which is the control input, given in (20), of the ith vehicle.

Remark 3. For the particular case of the interconnection between the leader and the first vehicle, we have

$$\Sigma_{1,0} : \begin{cases} \dot{x}_{1,i} = (A_1 + B_1 K_1) x_{1,i} + A_2 x_0 \\ \qquad\qquad + B_1 K_2 x_0(t_k) + E_1 e_{d,1} \\ \dot{x}_0 = A_0 x_{1,0} + D_0 u_0 + e_{d,0} \end{cases} \tag{27}$$

with $A_0 = -1/\tau_d$, $D_0 = -A_0$, and

$$z_1 = K_1 x_{1,1} + K_2 x_{2,0}(t_k). \tag{28}$$

In this case, we also have the input u_0 instead of ξ_0. Note also from (26) and (28) that the performance output z_i, for $i = 1, \dots, N$, is a linear combination of $x_{1,i} = [\Delta p_i \ \Delta v_i \ a_i \ u_i]^T$ and $x_{2,i-1} = [a_{i-1} \ u_{i-1}]^T$. Combined with the $\mathcal{L}_2$ stability analysis, this choice of z_i ensures that all variables involved in the platoon dynamics $\Sigma_{i,i-1}$ remain bounded with respect to the control input u_0 of the leader under zero initial conditions, thus ensuring string stability, as shown in (9).

Remark 4. Note that the overlapping system (25) is composed of the partial interconnection Σ_i with Σ_{i-1}. When combined, these overlapping systems $\Sigma_{i,i-1}$ describe the relationship from Σ_0 to Σ_i. This stacked dynamics has a block-diagonal structure, composed of the overlapping systems. Hence, evaluating the string stability and the individual vehicle stability of $\Sigma_{i,i-1}$ implies the stability of the platoon, allowing for *scalability* in the platoon setup.

C. Switched Dynamic Event-Triggering Mechanism

The feedforward component in the controller (20) is transmitted from vehicle Σ_{i-1} to vehicle Σ_i at time instants $\{t_k\}$, generated according to an ETM. To reduce the information transmission, we propose in the following a dynamic event-triggering condition. To this end, we define the error between the measured and the last transmitted states as

$$e_{x,i-1} = x_{2,i-1}(t) - x_{2,i-1}(t_k). \tag{29}$$

Then, the transmission from Σ_{i-1} to Σ_i occurs according to the following ETM:

$$\begin{aligned} t_{0,i} &= 0 \\ t_{k+1,i} &= \inf\{t > t_{k,i} + \varepsilon : \ \theta \Gamma(x_{2,i-1}, e_{x,i-1}) - \eta_i > 0\} \end{aligned} \tag{30}$$

where $\varepsilon > 0$ and $\theta > 0$ are design parameters, and

$$\Gamma(x_{2,i-1}, e_{x,i-1}) = e_{x,i-1}^T Q e_{x,i-1} - x_{2,i-1}^T R x_{2,i-1} \tag{31}$$

with Q and R symmetric positive definite matrices. The dynamic variable $\eta_i(t)$ is with the following switching dynamics:

$$\dot{\eta}_i = -\lambda_1 \eta_i (1 - \chi) - (\lambda_2 \eta_i + \Gamma(x_{2,i-1}, e_{x,i-1}))\chi \tag{32}$$

where $\eta_i(0) = 0$, and λ_1, λ_2 are positive scalars. The switching variable χ in (32) is defined as

$$\chi = \begin{cases} 0 & \text{for } t \in [t_k, t_k + \varepsilon] \\ 1 & \text{for } t \in [t_k + \varepsilon, t_{k+1}] \end{cases} \tag{33}$$

Note that the positive constant ε enforces a minimum waiting time between consecutive events, i.e., $t_{k+1} - t_k \geq \varepsilon$, to ensure Zeno-free behavior. Because of the enforced time ε, we divide the time interval between transmissions as

$$\mathcal{I}_0^k = [t_k, t_k + \varepsilon) \quad \text{and} \quad \mathcal{I}_1^k = [t_k + \varepsilon, t_{k+1}) \tag{34}$$

where $\mathcal{I}_0^k$ corresponds to the fixed time interval depending on ε, and $\mathcal{I}_1^k$ depends on the event-triggering condition.

Remark 5. The parameters λ_1 and λ_2 involved in the dynamics (32) can be set with small values to make the dynamic parameter $\eta_i(t)$ converges as slowly as possible and to reduce the number of events in the steady-state phase.

Based on the ETM (30) and the control input (20), the overlapping system (25) can be modeled according to the interval of interest. Defining $\tau(t) = t - t_k \leq \varepsilon$ as an *artificial* time delay related to the enforced minimum time, $x_i = \text{col}(x_{1,i}, x_{2,i-1})$, $w_{d,i} = \text{col}(e_{d,i}, e_{d,i-1})$, and

$$\begin{aligned} A &= \begin{bmatrix} A_1 & A_2 \\ 0 & A_3 \end{bmatrix}, \quad E = \begin{bmatrix} E_1 & 0 \\ 0 & E_2 \end{bmatrix}, \quad B = \begin{bmatrix} B_1 \\ 0 \end{bmatrix} \\ C_1 &= \begin{bmatrix} I & 0 \end{bmatrix}, \qquad C_2 = \begin{bmatrix} 0 & I \end{bmatrix}, \qquad D^T = \begin{bmatrix} D_1^T & 0 \end{bmatrix}. \end{aligned} \tag{35}$$

Then, the overlapping system $\Sigma_{i,i-1}$ in (25) can be rewritten in the following switching model:

$$\Sigma_{i,i-1}^{\chi} : \begin{cases} \dot{x}_i = (A + BK_1C_1)x + D\xi_{i-1} + Ew_{d,i} \\ \qquad + (1 - \chi) BK_2C_2 x(t - \tau) \\ \qquad + \chi BK_2(C_2 x - e_{x,i-1}) \\ z_i = K_1C_1x_i + (1 - \chi)K_2C_2x_i(t - \tau) \\ \qquad + \chi(C_2x_i - e_{x,i-1}) \end{cases} \tag{36}$$

where χ is defined in (33). Hence, during the fixed minimum time, where $t \in \mathcal{I}_0^k$, we have $\chi = 0$ and the system is denoted by $\Sigma_{i,i-1}^0$, while for $t \in \mathcal{I}_1^k$, we have $\chi = 1$ and the system is denoted by $\Sigma_{i,i-1}^1$.

D. Problem Formulation

Since the uncertainties of the nonhomogeneous platooning system (5) can be effectively compensated by the disturbance observer (13), the control gains K_1 and K_2 of controller (20) can be *a priori* chosen based on Remarks 1 and 2. However, these control gains can only ensure the string stability under continuous communication. For an event-triggering communication, the string stability and the individual vehicle stability can be lost because of the loss of synchrony. Also, since the platoon is not perfectly homogeneous due to the presence of $e_{d,i}$, this disturbance estimation error effects also need to be considered for stability analysis. Therefore, the platooning control problem is to design a control law (20) to ensure the distance policy between vehicles, i.e., $\Delta p_i \to 0$, such that the following specifications are verified.

- The individual vehicle stability is ensured in the ideal condition, i.e., homogeneity, linearity and continuous communication.
- The switching overlapping system (36) is $\mathcal{L}_2$ stable.
- The string stability is ensured in the sense of $\mathcal{L}_2$ stability, i.e., the vehicle inputs are constrained to be non-amplified over the whole nonhomogeneous platooning system.
- The number of transmissions between vehicles is reduced while ensuring the existence of a minimum time between triggering events, given by ε, to avoid Zeno behavior.

The following lemma asserts that $\eta_i(t)$, as defined in (32), remains non-negative for all $t \geq 0$. This property is crucial in constructing Lyapunov-Krasovskii functionals for the proofs in Section IV.

Lemma 1. Consider the variable $\eta(t)$, defined in (32), with $\eta(0) \geq 0$. Then, we have $\eta(t) \geq 0$, for all $t \geq 0$.

Proof. We distinguish the two following cases.
• *Case 1.* For $t \in \mathcal{I}_0^k$, it follows from (32) and (33) that $\dot{\eta} = -\lambda_1 \eta$. Then, it is clear that, for $\eta(t_k) \geq 0$, we have $\eta(t) \geq 0$, for $\forall t \in \mathcal{I}_0^k$.
• *Case 2.* For $t \in \mathcal{I}_1^k$, the event-triggering mechanism (30) imposes that $\Gamma < \eta/\theta$. Hence, combining with the dynamic equation $\dot{\eta} = -\lambda_2 \eta - \Gamma$ from (32), we have

$$\dot{\eta} \geq -\lambda_2 \eta - \frac{1}{\theta}\eta. \tag{37}$$

Then, by comparison lemma [49], it follows from (37) that, for $\eta(t_k + \varepsilon) \geq 0$, we have $\eta(t) \geq 0$, for $\forall t \in \mathcal{I}_1^k$.

Combining the results of the two above cases, and from the continuity of $\eta(t)$, it follows that, for $t_0 = 0$ and $\eta(0) \geq 0$, then we have $\eta(t) \geq 0$, for $\forall t \geq 0$. □

IV. Event-Triggered Platooning Control Design

This section presents our main results of switched dynamic $\mathcal{L}_2$ event-triggered control for vehicle platoons. The switched dynamic ETC design is recast as an optimization problem under LMI constraints. To begin with, we present the following proposition to account for the effect of uncertainty estimation errors in platooning stability analysis.

Proposition 1. Consider the overlapping system $\Sigma_{i,i-1}$ in (25) with $x_i(0) = 0$, and the performance output in (26). Assume that there exits an upper bound $w_{\max} > 0$ such that $\|w_{d,i}\|_{\mathcal{L}_2} \leq w_{\max}$, for all $i = 0, \ldots, N$. If there exist finite positive scalars β, β_0 and γ_0 such that

$$\|\xi_1\|_{\mathcal{L}_2} \leq \gamma_0 \|u_0\|_{\mathcal{L}_2} + \beta_0 \|w_{d,1}\|_{\mathcal{L}_2} \tag{38a}$$
$$\|\xi_i\|_{\mathcal{L}_2} \leq \|\xi_{i-1}\|_{\mathcal{L}_2} + \beta \|w_{d,i}\|_{\mathcal{L}_2} \tag{38b}$$

for all $i = 2, \ldots, N$. Then, we have

$$\|\xi_i\|_{\mathcal{L}_2} \leq \gamma_0 \|u_0\|_{\mathcal{L}_2} + ((i-1)\beta + \beta_0) e_{d,\max} \tag{39}$$

for all $i = 1, \ldots, N$.

Proof. By recursivity and using the expression (38a), we can derive from (38b) that

$$\|\xi_i\|_{\mathcal{L}_2} \leq \gamma_0 \|u_0\|_{\mathcal{L}_2} + \beta \sum_{j=2}^{i} \|w_{d,j}\|_{\mathcal{L}_2} + \beta_0 \|w_{d,1}\|_{\mathcal{L}_2}. \tag{40}$$

Since $\|w_{d,i}\|_{\mathcal{L}_2} \leq w_{\max}$, for $i = 1, \ldots, N$, then it follows that

$$\sum_{j=2}^{i} \|w_{d,j}\|_{\mathcal{L}_2} \leq \sum_{j=2}^{i} w_{\max} = (i-1) w_{\max}. \tag{41}$$

Combining (40) with (41), we obtain the expression (39). This completes the proof. □

Remark 6. Taking into account the disturbance estimation error, the inequality (38a) (respectively (38b)) in Proposition 1 ensures $\mathcal{L}_2$ stability between the leader Σ_0 and the vehicle Σ_1 (respectively the vehicle Σ_{i-1} and the vehicle Σ_i). For the case where $w_{d,i} \approx 0$, we can directly recover the string stability condition (9) in Definition 1 from (38a) and (38b) under zero initial condition.

Remark 7. Note from Proposition 1 that the disturbance caused by $w_{d,i} = \mathrm{col}(e_{d,i}, e_{d,i-1})$ is amplified according to the increased number of vehicles of the platoon. This means that achieving $\mathcal{L}_2$ stability is not possible for a nonhomogeneous platoon of infinite size. On the other hand, the $\mathcal{L}_2$ stability conditions depend on the upper bound $w_{\max}$, meaning that for small values of $w_{\max}$, more vehicles can be added without compromising the $\mathcal{L}_2$ gain performance. Moreover, the $\mathcal{L}_2$ stability conditions directly depend on the upper bound $w_{\max}$. This implies that the smaller the value of $w_{\max}$, the larger the number of vehicles that can be added to the platoon. With an effective DOB-based disturbance compensation, the bound $w_{\max}$ can be significantly reduced. In particular, when $e_{d,i} \to 0$, the number of vehicles of the platoon can be arbitrarily large.

A. Switched Dynamic ETC Design Conditions

The following theorem provides conditions to ensure the $\mathcal{L}_2$ stability of the switched overlapping system (36), as stated in Proposition 1.

Theorem 1. Consider the overlapping system $\Sigma_{i,i-1}^{\chi}$ in (36) and the event-triggered condition (30). For positive scalars δ, α, ε, if there exist positive scalars β, $\gamma \leq 1$, matrices P_1, P_2, X, X_1, Y_1, Y_2, Y_3 and symmetric matrices $P \succ 0$, $U \succ 0$, $Q \succ 0$ and $R \succ 0$ of appropriate dimensions such that the following optimization problem is feasible:

$$\min \mathrm{Tr}(Q) + \beta^2 \tag{42}$$
$$\Theta \succ 0, \quad \Psi \prec 0, \quad \Phi \prec 0, \quad \Omega \prec 0 \tag{43}$$
$$R - \delta I \succ 0 \tag{44}$$

where

$$\Theta = \begin{bmatrix} P + \varepsilon \Theta_{11} & \varepsilon \Theta_{12} \\ * & \varepsilon \Theta_{22} \end{bmatrix} \tag{45}$$

$$\Phi = \begin{bmatrix} \Phi_{11} & \Phi_{12} & \Phi_{13} & P_1 D & P_1 E & \Phi_{16} \\ * & \Phi_{22} & \Phi_{23} & P_2 D & P_2 E & 0 \\ * & * & \Phi_{33} & 0 & 0 & \Phi_{36} \\ * & * & * & -\gamma^2 I & 0 & 0 \\ * & * & * & * & -\beta^2 I & 0 \\ * & * & * & * & * & -I \end{bmatrix} \tag{46}$$

$$\Psi = \begin{bmatrix} \Psi_{11} & \Psi_{12} & \Psi_{13} & \Psi_{14} & P_1D & P_1E & \varepsilon Y_1^T \\ * & \Psi_{22} & \Psi_{23} & 0 & P_2D & P_2E & \varepsilon Y_2^T \\ * & * & \Psi_{33} & \Psi_{34} & 0 & 0 & \varepsilon Y_3^T \\ * & * & * & -I & 0 & 0 & 0 \\ * & * & * & * & -\gamma^2 I & 0 & 0 \\ * & * & * & * & * & -\beta^2 I & 0 \\ * & * & * & * & * & * & \Psi_{77} \end{bmatrix} \quad (47)$$

$$\Omega = \begin{bmatrix} \Omega_{11} & \Omega_{12} & \Omega_{13} & P_1D & P_1E & K^T \\ * & \Omega_{22} & \Omega_{23} & P_2D & P_2E & 0 \\ * & * & -Q & 0 & 0 & -K_2^T \\ * & * & * & -\gamma^2 I & 0 & 0 \\ * & * & * & * & -\beta^2 I & 0 \\ * & * & * & * & * & -I \end{bmatrix} \quad (48)$$

with

$\Theta_{11} = \frac{X+X^T}{2}$, $\Theta_{12} = X_1 - X$, $\Theta_{22} = -X_1 - X_2^T + \Theta_{11}$
$\Psi_{11} = \mathrm{He}\{(A + BK_1C_1)^T P_1^T\} + 2\alpha P - Y_1 - Y_1 - \Theta_{11}$
$\Psi_{12} = (A + BK_1C_1)^T P_2^T - P_1 + P - Y_2^T$
$\Psi_{13} = P_1BK_2C_2 + Y_1 - Y_3^T + \Theta_{12}$, $\Psi_{14} = \Phi_{16} = C_1^T K_1^T$
$\Psi_{22} = N_{22} = -P_2 - P_2^T$, $\Psi_{23} = P_2BK_2C_2 + Y_2$
$\Psi_{33} = Y_3 + Y_3^T + \Theta_{22}$, $\Psi_{34} = \Phi_{36} = C_2^T K_2^T$
$\Psi_{77} = -Te^{-2\alpha}U$, $\Phi_{11} = \Psi_{11} + 2\alpha\varepsilon\Theta_{11}$
$\Phi_{12} = \Psi_{12} + \varepsilon\Theta_{11}$, $\Phi_{13} = \Psi_{13} + 2\alpha\varepsilon\Theta_{12}$
$\Phi_{22} = \Psi_{22} + U$, $\Phi_{23} = \Psi_{23} + \varepsilon\Theta_{12}$, $\Phi_{33} = \Psi_{33} + 2\alpha\varepsilon\Theta_{22}$
$\Omega_{11} = \mathrm{He}\{(A + BKC)^T P_1^T\} + 2\alpha P + C_2^T R C_2$
$\Omega_{12} = (A + BK_1C_1)^T P_2^T - P_1$
$\Omega_{13} = P_1BK_2$, $\Omega_{23} = P_2BK_2$.

Then, the overlapping system $\Sigma_{i,i-1}^{\chi}$ in (25) is stable under the event-triggering condition (30). Moreover, the dynamics of η is stable and condition (38b) in Proposition 1 holds for system (25) with an $\mathcal{L}_2$ gain less than or equal to β.

Proof. For brevity, we omit the subscript i in x_i, z_i, $e_{x,i-1}$, ξ_{i-1} and $w_{d,i}$. For the stability analysis of system (25), we consider the Lyapunov-Krasovskii functional candidate

$$V^{\chi}(x,\eta) = W(x,\eta) + (1-\chi)(V_1 + V_2) \quad (49)$$

with $W(x,\eta) = x^T P x + \eta$, and

$$V_1 = (\varepsilon - \tau(t)) \begin{bmatrix} x \\ x(t_k) \end{bmatrix}^T \begin{bmatrix} \Theta_{11} & \Theta_{12} \\ * & \Theta_{22} \end{bmatrix} \begin{bmatrix} x \\ x(t_k) \end{bmatrix} \quad (50)$$

$$V_2 = (\varepsilon - \tau(t)) \int_{t-\tau(t)}^{t} e^{2\alpha(s-t)} \dot{x}^T(s) U \dot{x}(s) ds. \quad (51)$$

Note that at switching instants t_k and $t_k + \varepsilon$, i.e., $\tau(t) = 0$ and $\tau(t) = \varepsilon$ respectively, $V^{\chi}(x,\eta) = W(x,\eta) = V^1(x,\eta)$. This implies that the functional $V^{\chi}(x,\eta)$ is continuous for all $t \geq 0$. Considering the definition of Θ in (45), then condition

$$\frac{\varepsilon - \tau(t)}{\varepsilon}\Theta + \frac{\tau(t)}{\varepsilon} \begin{bmatrix} P & 0 \\ * & 0 \end{bmatrix} \succeq 0 \quad (52)$$

implies $x^T P x + V_1 \geq 0$. Note also that to ensure (52), it suffices to impose $\Theta \succ 0$ and $P \succ 0$. Since $V_2 \geq 0$ by construction in (51) and $\eta \geq 0$ from Lemma 1, for $\forall t \geq 0$, then $V^{\chi}(x,\eta)$ in (49) is a proper LKF candidate.

Due to the switching nature of the proposed dynamic ETC approach, in the subsequent part of the proof, we first consider two cases, corresponding to the two time intervals $\mathcal{I}_0^k$ and $\mathcal{I}_1^k$, defined in (34). Then, we combine the two intervals as $[t_k, t_{k+1}] = \mathcal{I}_0^k \cup \mathcal{I}_1^k$ for stability analysis.

1) System $\Sigma_{i,i-1}^0$ and $t \in \mathcal{I}_0^k$: For this time interval, one has $V^0(x,\eta) = W(x,\eta) + V_1 + V_2$. We compute

$$\dot{W}(x,\eta) = \dot{x}^T P x + x^T P \dot{x} - \lambda_1 \eta \quad (53)$$

$$\dot{V}_1 = -\begin{bmatrix} x \\ x(t_k) \end{bmatrix}^T \begin{bmatrix} \Theta_{11} & \Theta_{12} \\ * & \Theta_{22} \end{bmatrix} \begin{bmatrix} x \\ x(t_k) \end{bmatrix} + (\varepsilon - \tau(t))\dot{x}[2\Theta_{11}x + 2\Theta_{12}x(t_k)] \quad (54)$$

$$\dot{V}_2 \leq -2\alpha V_2 - e^{2\alpha\varepsilon} \int_{t-\tau(t)}^{t} \dot{x}(s)^T U \dot{x}(s) ds + (\varepsilon - \tau(t))\dot{x}^T U \dot{x}. \quad (55)$$

Let us define $\kappa(t) = \frac{1}{\tau(t)} \int_{t-\tau(t)}^{t} \dot{x}(s) ds$. Then, using the Jensen's inequality [45], it follows that

$$-e^{2\alpha\varepsilon} \int_{t-\tau(t)}^{t} \dot{x}(s)^T U \dot{x}(s) ds \leq -\tau(t) e^{2\alpha\varepsilon} \kappa(t)^T U \kappa(t) \quad (56)$$

Moreover, we have $x(t) = x(t_k) + \tau(t)\kappa(t)$. Then, for any matrices Y_1, Y_2 and Y_3 of suitable dimensions, it follows that

$$0 = \mathrm{He}\{(x^T Y_1 + \dot{x}^T Y_2 + x^T(t_k) Y_3)[x(t_k) - x + \tau\kappa]\} \quad (57)$$

Similarly, from the expressions of $\dot{x}$ and z in (36) for $t \in \mathcal{I}_0^k$, we can directly obtain the following null terms:

$$0 = \mathrm{He}\{(x^T P_1 + \dot{x}^T P_2)[(A + BK_1C_1)x + BK_2C_2x(t_k) + D\xi + Ew_d - \dot{x}]\} \quad (58)$$

$$0 = \mathrm{He}\{z^T[K_1C_1x + K_2C_2x(t_k) - z]\}. \quad (59)$$

Combining (53), (54), (55), the inequality (56), the performance output z in (36), and adding the null terms (57), (58) and (59), we can derive the following inequality:

$$\dot{V}^0 + 2\alpha V^0(x,0) + \lambda_1\eta + z^T z - \gamma^2 \xi^T \xi - \beta^2 w_d^T w_d \leq \mu_0^T \mathcal{L}(\tau(t)) \mu_0 \quad (60)$$

where $\mu_0 = \mathrm{col}(x, \dot{x}, x(t_k), \xi, w_d, z, \kappa)$. The matrix $\mathcal{L}(\tau(t))$ is affine on $\tau(t)$, which can be expressed as

$$\mathcal{L}(\tau(t)) = \frac{\tau(t)}{\varepsilon}\Psi + \frac{\varepsilon - \tau(t)}{\varepsilon} \begin{bmatrix} \Phi & 0 \\ * & 0 \end{bmatrix} \quad (61)$$

where Φ and Ψ are defined in (46) and (47), respectively. Note from (61) that the conditions $\Phi \prec 0$ and $\Psi \prec 0$ from (43) ensure that $\mathcal{L}(\tau(t)) \preceq 0$, for all $\tau(t) \in (0, \varepsilon]$.

2) System $\Sigma^1_{i,i-1}$ and $t \in \mathcal{I}^k_1$: For this time interval, we have $V^\chi(x,\eta) = W(x,\eta)$. Taking its time derivative yields

$$\dot{V}^1 = \dot{x}^T P x + x^T P \dot{x} + x^T C_2^T R C_2 x - e^T_{x,i-1} Q e_{x,i-1} - \lambda_2 \eta. \quad (62)$$

As in the previous case, we can derive the following equalities from (36) for $t \in \mathcal{I}^k_1$:

$$0 = \mathrm{He}\{(x^T P_1 + \dot{x}^T P_2)[(A+BKC)x + BK_2 e_{x,i-1} + D\xi + E w_d - \dot{x}]\} \quad (63)$$

$$0 = \mathrm{He}\{z^T[KCx + K_2 e_{x,i-1} - z]\}. \quad (64)$$

Adding the null terms in (63) and (64) to (62), we can derive

$$\dot{V}^1 + 2\alpha V^1(x,0) + \lambda_2 \eta + z^T z - \gamma^2 \xi^T \xi - \beta^2 w_d^T w_d \leq \mu_1^T \Omega \mu_1 \quad (65)$$

where $\mu_1^T = (x, \dot{x}, e_{x,i-1}, \xi, w_d, z)$, and Ω is defined in (48). Hence, the condition $\Omega \prec 0$ in (43) ensures that $\mu_1^T \Omega \mu_1 \leq 0$.

3) System $\Sigma^\chi_{i,i-1}$ and $t \geq 0$: Since $[t_k, t_{k+1}] = \mathcal{I}^k_0 \cup \mathcal{I}^k_1$, combining the conditions (60) and (62), it follows that

$$\dot{V}^\chi + 2\alpha V^\chi(x,0) + \min\{\lambda_1, \lambda_2\}\eta + z^T z - \gamma^2 \xi^T \xi - \beta^2 w_d^T w_d \leq 0 \quad (66)$$

for $\forall t \in \cup_{k=0}^{\infty}[t_k, t_{k+1}]$. For $\mathrm{col}(\xi, w_d) \neq 0$, condition (66) implies that $\dot{V}^\chi + z^T z - \gamma^2 \xi^T \xi - \beta^2 w_d^T w_d \leq 0$. Integrating this latter from 0 to ∞, it follows that

$$V^\chi|_{t\to\infty} - V^\chi|_{t\to 0} + \|z\|^2_{\mathcal{L}_2} - \gamma^2 \|\xi\|^2_{\mathcal{L}_2} - \beta^2 \|w_d\|^2_{\mathcal{L}_2} \leq 0. \quad (67)$$

From the definition of the LKF in (49), we have that $V(\chi) \geq 0$, for all $t \geq 0$. Hence, condition (67) implies that

$$\|z\|_{\mathcal{L}_2} \leq \gamma \|\xi\|_{\mathcal{L}_2} + \beta \|w_d\|_{\mathcal{L}_2} + \sqrt{V^\chi|_{t\to 0}}. \quad (68)$$

Under zero initial conditions, since $\gamma \leq 1$ we can recover from (68) the condition (38b) in Proposition 1.

Moreover, the LMI constraint (44) and the minimization of $\mathrm{Tr}(Q)$ in (42) are used to maximize the inter-event time of the switched dynamic ETC scheme. This completes the proof. □

Remark 8. For the $\mathcal{L}_2$ stability of the leader vehicle Σ_0, the condition (38a) in Proposition 1 can be satisfied with Theorem 1 by using the $\Sigma_{1,0}$ dynamics (27) while removing the restriction $\gamma \leq 1$.

Remark 9. The static event-triggering mechanism can be directly retrieved from Theorem 1 by making $\theta \to \infty$ in (30), which results in

$$\begin{aligned} t_{0,i} &= 0 \\ t_{k+1,i} &= \inf\{t > t_{k,i} + \varepsilon : \ \Gamma(x_{2,i-1}, e_{x,i-1}) > 0\} \end{aligned} \quad (69)$$

where $\Gamma(x_{2,i-1}, e_{x,i-1})$ is defined in (31).

Remark 10. An alternative to the time gap distance policy in (8) can be considered as $\Delta p_{r,i} = r_i + h_i v_i$, where h_i can also vary according to the vehicle. In this case, the overlapping system $\Sigma_{i,i-i}$ in (25) depends on both h_i and h_{i-1}. Specifically, we will have matrices A_1, B_1, D_1 depending on h_i, i.e., $A_1(h_i)$, $B_1(h_i)$, $D_1(h_i)$, and matrix A_3 depending on h_{i-1}, i.e., $A_3(h_{i-1})$. Therefore, the design conditions in Theorem 1 must be evaluated considering $A_1(h_i)$, $B_1(h_i)$, $D_1(h_i)$, and $A_3(h_{i-1})$ for each h_i and h_{i-1}. In this paper, we assume a constant parameter h in (8) to ensure the direct scalability of the proposed string stability conditions.

B. Periodic ETC Design Conditions

To show the generic feature of the proposed ETC method and for comparison purposes, we provide an adaptation of Theorem 1 to the case of static periodic ETC design. To this end, we consider the following event-triggering mechanism:

$$\begin{aligned} t_{k+1,i} = \inf\{&t_{k,i} + j\varepsilon : \ j \in \mathbb{N}, \\ &x^T_{2,i-1}(t_{k,i} - j\varepsilon) R x_{2,i-1}(t_{k,i} - j\varepsilon) - e^T_{x,i-1} Q e_{x,i-1} > 0\} \end{aligned} \quad (70)$$

with $e_{x,i-1} = x_{2,i-1}(t_{k,i} - j\varepsilon) - x_{2,i-1}(t_{k,i})$. Let us define $\tau(t) = t - t_{k,i} - j\varepsilon$, then the switching overlapping system (36) can be recast as

$$\begin{aligned} \dot{x} &= (A + BK_1C_1)x + BK_2C_2 x(t-\tau(t)) - BK_2 e_{x,i-1} + D\xi_{i-1} + E w_d \\ z &= K_1C_1 x + K_2C_2 x(t-\tau(t)) - K_2 e_{x,i-1}. \end{aligned} \quad (71)$$

Based on system (71) and the event-triggering condition (70), we provide the following theorem for periodic ETC design.

Theorem 2. For positive scalars δ, α, ε, if there exist positive scalars β, $\gamma \leq 1$, matrices P_1, P_2, X, X_1, Y_1, Y_2, Y_3, and symmetric matrices $P \succ 0$, $U \succ 0$, $Q \succ 0$ and $R \succ 0$ of appropriate dimensions such that the following optimization problem is feasible:

$$\min \mathrm{Tr}(Q) + \beta \quad (72)$$

$$H_0 \succ 0, \quad R - \delta I \succ 0 \quad (73)$$

$$\tilde{\Phi} = \begin{bmatrix} \bar{\Phi} & \Xi \\ * & -Q \end{bmatrix} \prec 0, \quad \tilde{\Psi} = \begin{bmatrix} \bar{\Psi} & \Xi \\ * & -Q \end{bmatrix} \prec 0 \quad (74)$$

with

$$\bar{\Phi}_{22} = \Phi_{22} + C^T R C, \qquad \bar{\Psi}_{22} = \Psi_{22} + C^T R C$$
$$\bar{\Phi}_{ij} = \Phi_{ij}, \qquad \bar{\Psi}_{ij} = \Psi_{ij}$$
$$\Xi = \begin{bmatrix} K_2^T B^T P_1 & K_2^T B^T P_2 & 0 & \dots & -K_2^T \end{bmatrix}^T.$$

Then, the closed-loop system (71) is stable under the periodic ETM (70). Moreover, condition (38b) in Proposition 1 holds for system (71) with an $\mathcal{L}_2$ gain less than or equal to β.

Proof. We provide a sketch of this proof in the following since it follows similar steps to that of Theorem 1. Choosing the Lyapunov function candidate $V = x^T P x + V_1 + V_2$, and considering the same time derivatives as in (54) and (55), and the following null terms:

$$0 = \mathrm{He}\{(x^T P_1 + \dot{x}^T P_2)[(A+BK_1C_1)x + BK_2C_2 x(t-\tau) - BK_2 e_{x,i-1} + D\xi + E w_d - \dot{x}]\}$$
$$0 = \mathrm{He}\{z^T[K_1C_1 x + K_2C_2 x(t-\tau) - K_2 e_{x,i-1} - z]\}$$

along with (57), as in the proof of Theorem 1, we can derive

$$\dot{V} + 2\alpha V + x^T C_2^T R C_2 x - e^T_{x,i-1} Q e_{x,i-1} + z^T z - \gamma^2 \xi^T \xi - \beta^2 w_d^T w_d \leq \tilde{\mu}^T \mathcal{H}(\tau(t)) \tilde{\mu} \quad (75)$$

with $\tilde{\mu} = \text{col}(x, \dot{x}, x(t_k), \kappa, \xi, w_d, z, e_{x,i-1})$, and

$$\mathcal{H}(\tau(t)) = \frac{\tau(t)}{\varepsilon}\tilde{\Psi} + \frac{\varepsilon - \tau(t)}{\varepsilon}\begin{bmatrix}\tilde{\Phi} & 0\\ * & 0\end{bmatrix} \tag{76}$$

for $\tau(t) \in (0, \varepsilon]$, where the matrices $\tilde{\Psi}$ and $\tilde{\Phi}$ are defined in (74). Note that the matrix $\mathcal{H}(\tau(t))$ is affine in $\tau(t)$, and condition (74) ensures that

$$\tilde{\mu}^T \mathcal{H}(\tau(t))\tilde{\mu} \leq 0. \tag{77}$$

Note also that the ETM (70) ensures that

$$x(t-\tau)^T C_2^T R C_2 x(t-\tau) - e_{x,i-1}^T Q e_{x,i-1} < 0. \tag{78}$$

For $\text{col}(\xi, w_d) \neq 0$, it follows from (75), (77) and (78) that

$$\dot{V} + 2\alpha V + z^T z - \gamma^2 \xi^T \xi - \beta^2 w_d^T w_d \leq 0. \tag{79}$$

Integrating the condition (79) from 0 to ∞, we can obtain (38b). This completes the proof. □

Remark 11. For the choice of the control design parameters in Theorems 1 and 2, the maximum time parameter ε is chosen such that the ETC design conditions are feasible without compromising the $\mathcal{L}_2$ gain β. The parameter δ is searched to maximize the inter-event times, i.e., to increase the norm-value of R. The maximum decay rate α is chosen to ensure a fast closed-loop convergence while guaranteeing the feasibility of the ETC design conditions.

V. Illustrative Results and Comparisons

This section presents illustrative results and various comparative studies to show the effectiveness of the proposed switched dynamic ETC platooning control method. To corroborate the proposed control approach this end, we consider a platoon setup with one leader (Σ_0) and four followers (Σ_1 to Σ_4). For each follower, the nominal parameters are different. Table II presents the nominal values of the vehicle parameters and their corresponding uncertainties, denoted by Δ_i, as a percentage for each vehicle with $i = 0, 1, 2, 3, 4$, which results in a nonhomogeneous platoon setup. For simulations, the rolling resistance coefficient F_r is considered constant for all vehicles, i.e., $F_r = 0.015$ (s/kg). However, it is assumed to be unknown and is not used to compute the feedback linearizing control law (15). Moreover, the length of the vehicles, $L_c = 2.5$ (m), is also known for all vehicles.

For all vehicles, the feedback linearizing controller (15) is designed considering the nominal vehicle values, i.e., the columns Σ_i in Table II. For DOB-based disturbance compensation, we compute $\hat{d}_i$ in (15) using the disturbance observer (13) with $L(a_i) = La_i$. The DOB gain L as well as the distance policy parameters from (8) and the desired time constant τ_d are given in Table III. The feedback gains K_1 and K_2 of the control law (20) are chosen following Remarks 1 and 2 as[1]

$$K_1 = \begin{bmatrix}0.2 & 0.7 & -0.42 & 0\end{bmatrix}, \quad K_2 = \begin{bmatrix}-0.2 & 1.2\end{bmatrix}.$$

[1]Note that the feedback gain K_1 is chosen to be the same as in [14] for the comparison between different ETMs in Subsection V-C, while the feedforward gain K_2 can be easily selected to fulfill (24).

TABLE II: Nominal values of the vehicle parameters and respective uncertainties in percentage.

Par.	Σ_0	Δ_0	Σ_1	Δ_1	Σ_2	Δ_2	Σ_3	Δ_3	Σ_4	Δ_4
m	1724	0 %	2241	-10%	2930	-10%	3620	-10%	3965	50%
h_w	0.276	-10%	0.635	-20%	0.414	-20%	0.635	40%	0.524	20%
J_r	0.748	40%	0.972	-30%	1.571	-20%	0.823	40%	1.720	40%
J_e	0.140	00%	0.350	30%	0.266	50%	0.266	50%	0.238	20%
R_g	0.104	20%	0.177	00%	0.198	50%	0.115	-30%	0.115	20%
b	7.350	10%	13.965	-20%	11.025	-20%	13.965	10%	8.085	40%
c	0.190	20%	0.437	40%	0.285	-30%	0.399	50%	0.209	50%
τ	0.050	50%	0.095	-10%	0.075	-20%	0.125	0 %	0.075	50%

TABLE III: Distance policy, DOB gain and ETC parameters.

Par.	$r_{[1,2,3,4]}$	h	τ_d	L	ε	δ	α	θ	λ_1	λ_2
Value	2	0.6	0.1	50	0.1	0.005	0.01	5	0.01	0.01

A. Test 1: DOB-Based Disturbance Compensation

This test is used to evaluate the control performance and highlight the importance of DOB-based uncertainty compensation for a nonhomogeneous platoon. To this end, the simulations are performed for two cases: uncertain platoon with and without DOB-based uncertainty compensation, without considering the effects of the ETC. For this test, the vehicles follow the leader with a velocity v_0, as shown in Fig. 3. For all the followers, the initial conditions are chosen as $[\Delta p_i \ \Delta v_i \ a_i \ u_i] = 0$, i.e., all the vehicles are stationary and with a correct distance policy.

Fig. 3 shows the difference in distance policy for two cases: i) platoon without uncertainty (nominal), ii) uncertain platoon with DOB-based uncertainty compensation (uncertainty with DOB). Observe that the DOB is able to compensate for disturbances, resulting in a platooning control behavior similar to the nominal case. The vehicles exhibit behaviors close to the nominal, forming a nearly homogeneous platoon. The importance of the DOB becomes more evident when compared with the case without uncertainty compensation, as shown in Fig. 4. In this scenario, the distance policy error is on the order of 10 meters, which can be considered dangerous and may lead to collisions in practical situations.

B. Test 2. Performance Evaluation of Switched Dynamic ETC

This test is used to evaluate the tracking control performance of the proposed switched dynamic ETC design with and without DOB-based disturbance compensation. With the same chosen control gains K_1 and K_2 as in Test 1 and the control parameters given in Table III, the event-triggering condition (30) is designed using Theorem 1. The optimization problem (42) results in $\beta = 2.5$, and

$$Q = \begin{bmatrix}2.77 & -16.61\\ * & 99.65\end{bmatrix}, \quad R = \begin{bmatrix}0.0145 & -0.0132\\ * & 0.0143\end{bmatrix}. \tag{80}$$

Fig. 5 shows the velocity v, the acceleration a, and the distance policy error Δp for each vehicle in the considered nonhomogeneous platoon. Note that the vehicles in the platoon are able to follow the leader velocity and the distance policy converges to zero without significant oscillations. Moreover,

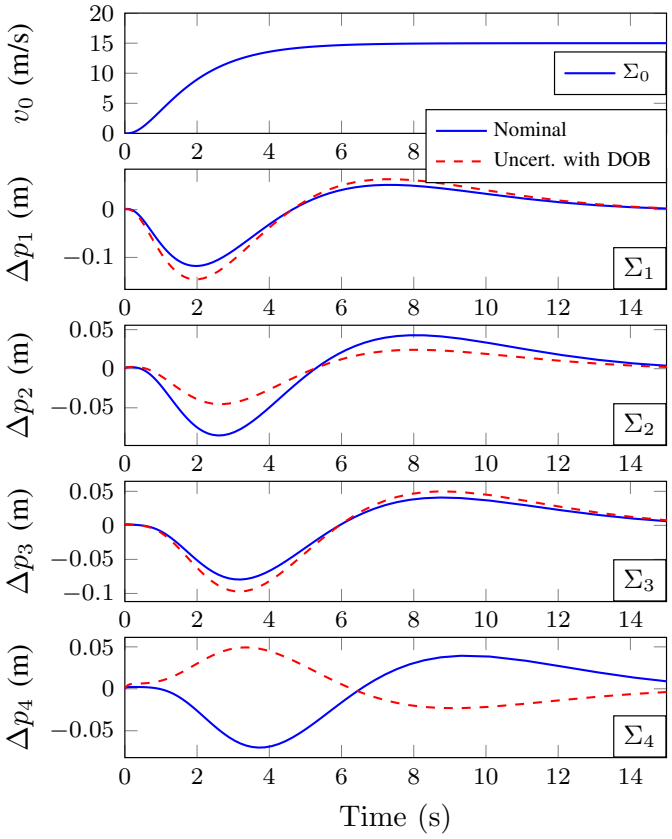

Fig. 3: Test 1. Comparison between the nominal platoon and the uncertain platoon with DOB-based uncertainty compensation for continuous communication.

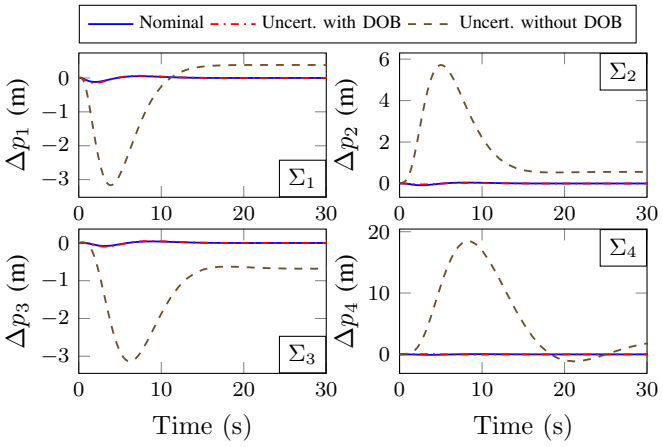

Fig. 4: Test 1. Comparison of distance policy errors Δp_i between the nominal platoon and the uncertain platoon with and without DOB-based uncertainty compensation for continuous communication.

employing the same event-triggering control mechanism, we compare the distance policy errors between vehicles obtained with and without DOB-based disturbance compensation. As seen in Fig. 6, there is a significant difference in the distance policy errors, reaching values on the order of 10 (m), for the case without disturbance compensation.

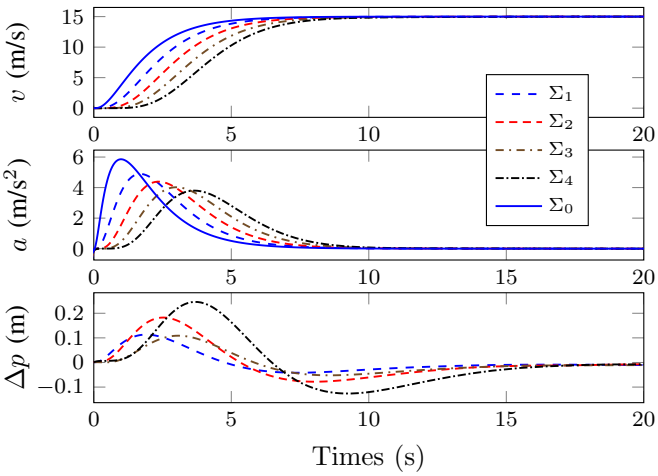

Fig. 5: Test 2. Velocity v, acceleration a and distance policy error Δp of the platooning vehicles obtained with the switched dynamic ETM (30), designed based on Theorem 1.

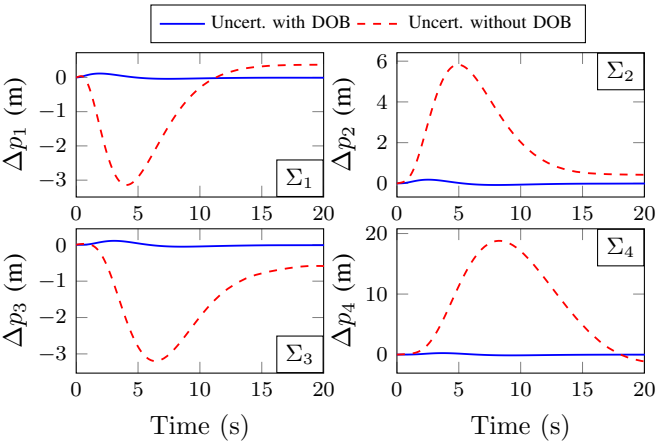

Fig. 6: Test 2. Distance policy errors Δp_i obtained with the switched dynamic ETM, designed based on Theorem 1, with and without DOB-based uncertainty compensation.

Now considering a time-varying velocity reference for a longer simulation time interval of $t_{\text{sim}} = 320$ (s), as illustrated in Fig. 7. We observe that the follower vehicles can still correctly follow the leader and maintain the specified distance policy. Fig. 7 also displays the inter-event time for transmissions to vehicles Σ_1 to Σ_4. Notice that every time the leader changes its velocity, the inter-event time is reduced. However, as the vehicles reach a steady state, the number of transmissions considerably decreases, as evident in the last steady state after 220 seconds.

C. Test 3. Comparison between Different ETC Mechanisms

To further evaluate the platooning control performance, we compare the four following ETMs under the same test conditions as in Fig. 5:

- Proposed dynamic ETM, designed with Theorem 1.

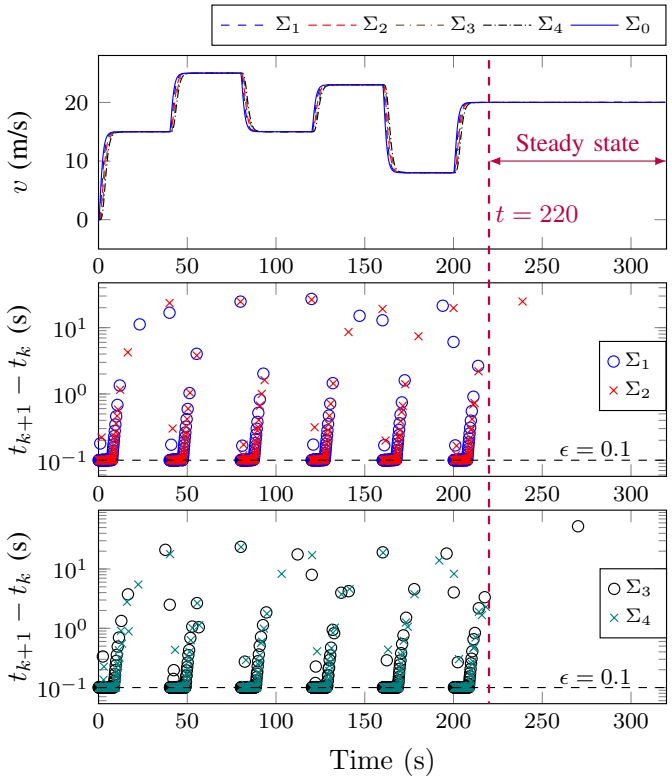

Fig. 7: Test 2. Platooning with a time-varying velocity reference, and inter-event time for each vehicle obtained with the switched dynamic ETC design from Theorem 1.

- Dynamic ETM, proposed in [14]. Following the same search procedure as in [14], the parameters of the ETM can be determined, as depicted in Table IV.[2]
- Static ETM, discussed in Remark 9.
- Periodic ETM, designed with Theorem 2.

TABLE IV: ETM parameters obtained for the ETM in [14].

Parameter	γ	τ_{meit}	$\phi_1(0)$	ϵ	λ	ρ
Value	8.442	0.1	2.8674	0.5	0.2027	0.04

In Fig. 8, we observe that the distance policy errors do not show significant differences among the considered event-triggering mechanisms. However, in terms of communication, there is a significant difference, as shown in Table V, which summarizes the average time between events during the transient phase T_{avg}, and the number of events N_{event} obtained with the four ETC schemes. In particular, the switched dynamic ETC scheme shows a significant difference compared to the other cases, with almost less than a third of the number of events. Furthermore, in Table V, we present the ratio of total simulation time to the number of events, denoted as $T_{\text{sim}}/N_{\text{event}}$, with $T_{\text{sim}} = 320$ (s). When comparing this value with T_{avg}, a significant difference is observed only in the proposed switched dynamic ETC scheme. This is mainly due to the long interval without triggering communication, which is not included in the average. Furthermore, it is noteworthy that in the presence of parametric uncertainties and exogenous disturbances, the dynamic ETC method presented in [14] yields a control performance similar to that of the compared static ETC scheme. To better illustrate this difference in triggering communication, Fig. 9 depicts the inter-event times obtained with different ETMs. We can clearly see that, except for the proposed method, the numbers of events of other compared ETMs do not reduce as the platooning system achieves the steady state, and the transmission intervals are close to the minimum time. This confirms the advantages of the proposed ETC method in comparison to related results.

[2]Note that with the ETM parameters provided in Table IV, both the proposed method and the one in [14] yield similar ETC performance for platooning systems without parametric uncertainties and exogenous disturbances, although these results are not shown here for brevity.

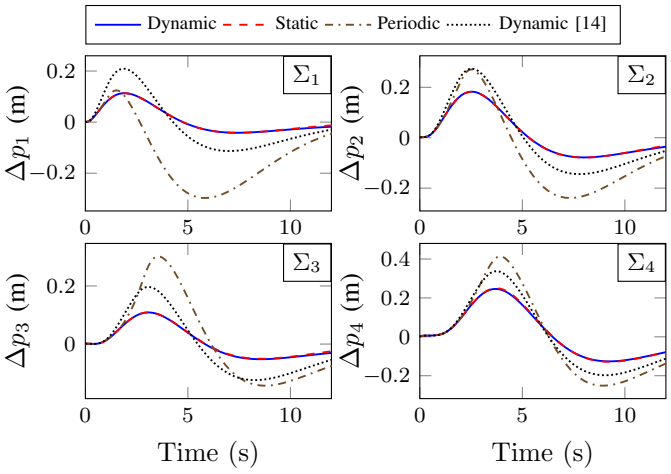

Fig. 8: Test 3. Distance policy errors Δp_i obtained using the four compared ETMs.

TABLE V: Average time between events during the transient phase T_{avg}, number of events N_{event}, and average events during the total simulation time $T_{\text{sim}}/N_{\text{event}}$ obtained with four ETC schemes.

ETC	Indicator	Vehicle			
		1	2	3	4
Dynamic	T_{avg} (s)	0.40	0.38	0.37	0.35
	N_{event}	534	559	589	617
	$T_{\text{sim}}/N_{\text{event}}$	0.60	0.57	0.54	0.52
Static	T_{avg} (s)	0.10	0.11	0.11	0.11
	N_{event}	3004	2817	2606	2729
	$T_{\text{sim}}/N_{\text{event}}$	0.11	0.11	0.12	0.12
Periodic	T_{avg} (s)	0.20	0.22	0.23	0.23
	N_{event}	1953	1701	1385	1439
	$T_{\text{sim}}/N_{\text{event}}$	0.16	0.19	0.23	0.22
[14]	T_{avg} (s)	0.11	0.11	0.11	0.11
	N_{event}	2954	2912	2843	2885
	$T_{\text{sim}}/N_{\text{event}}$	0.11	0.11	0.11	0.11

VI. Concluding Remarks

Considering the control communication between vehicles in the predecessor-follower flow topology, a switched dynamic ETC method has been proposed for nonhomogeneous platoons. To effectively compensate for the uncertainties of

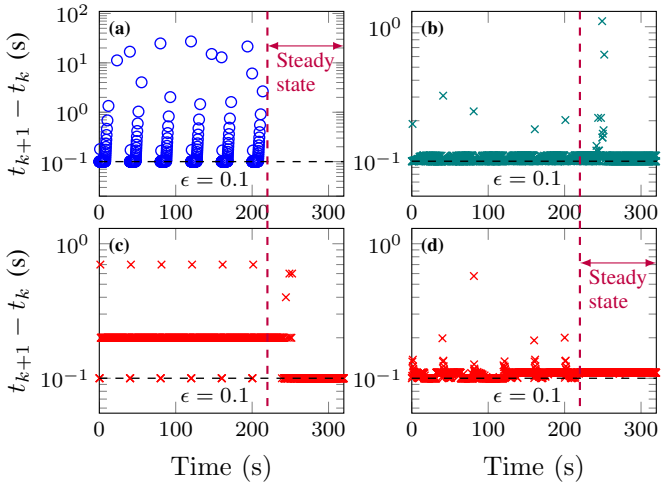

Fig. 9: Test 3. Inter-event times obtained using the four compared ETMs. (a) Proposed dynamic ETM, (b) Static ETM, (c) Periodic ETM, (d) Dynamic ETM [14].

the platooning system, treated as a virtual disturbance, a DOB-based uncertainty estimate is included in the feedback linearization control law. As a result, string stability and the stability of individual vehicles can be evaluated in a manner similar to the classical CACC design conditions. The control communication between vehicles is established based on a dynamic event-triggering condition with a minimum time to ensure Zeno-free behavior. For platooning control, from the vehicle dynamics and using a switching modeling technique, we form an overlapping system $\Sigma_{i,i-1}$, representing the interconnection between two adjacent vehicles Σ_i and Σ_{i-1}. Subsequently, using a Lyapunov-Krasovskii functional and the null-term relaxation technique, sufficient LMI conditions are derived to ensure $\mathcal{L}_2$ stability between the vehicle systems Σ_i and Σ_{i-1}, as well as $\mathcal{L}_2$ string stability for a limited-size platoon, considering the disturbance estimation error as an additional exogenous input. Through extensive simulations and comparisons, we demonstrate that the proposed DOB-based event-triggered platooning control method can ensure string stability despite the presence of considerable modeling uncertainties. Furthermore, the dynamic switched ETC can also reduce the amount of communication compared to static ETC and periodic ETC mechanisms, ensuring long time intervals without transmissions when the nonhomogeneous platoon achieves the steady state. Due to the generic formulation of the proposed ETC platooning control method with LKF-based stability analysis, the $\mathcal{L}_2$ design conditions can be further extended in the future to consider time delays, actuator faults, and attacks. Extensions to different communication topologies will also be investigated, exploiting the particularities of each while maintaining the scalability of the $\mathcal{L}_2$ design conditions.

References

[1] J. Guanetti, Y. Kim, and F. Borrelli, "Control of connected and automated vehicles: State of the art and future challenges," *Annu. Rev. Control.*, vol. 45, p. 18–40, 2018.

[2] Y. Bian, Y. Zheng, W. Ren, S.-E. Li, J. Wang, and K. Li, "Reducing time headway for platooning of connected vehicles via V2V communication," *Transp. Res. Part C Emerg. Technol.*, vol. 102, pp. 87–105, 2019.

[3] J. Chen, H. Wei, H. Zhang, and Y. Shi, "Asynchronous self-triggered stochastic distributed MPC for cooperative vehicle platooning over vehicular ad-hoc networks," *IEEE Trans. Veh. Technol.*, vol. 72, no. 11, pp. 14 061–14 073, 2023.

[4] A. Johansson, T. Bai, K. H. Johansson, and J. Mårtensson, "Platoon cooperation across carriers: From system architecture to coordination," *IEEE Intell. Transp. Syst. Mag.*, vol. 15, no. 3, p. 132–144, 2023.

[5] T. Bai, A. Johansson, K. H. Johansson, and J. Mårtensson, "Large-scale multi-fleet platoon coordination: A dynamic programming approach," *IEEE Trans. Intell. Transp. Syst.*, vol. 24, no. 12, p. 4427–4442, 2023.

[6] W. Bai, B. Xu, H. Liu, Y. Qin, and C. Xiang, "Robust longitudinal distributed model predictive control of connected and automated vehicles with coupled safety constraints," *IEEE Trans. Veh. Technol.*, vol. 72, no. 3, pp. 2960–2973, 2023.

[7] D. Jia, K. Lu, J. Wang, X. Zhang, and X. Shen, "A survey on platoon-based vehicular cyber-physical systems," *IEEE Commun. Surv. Tutor.*, vol. 18, no. 1, pp. 263–284, 2016.

[8] S. Feng, Y. Zhang, S. E. Li, Z. Cao, H. X. Liu, and L. Li, "String stability for vehicular platoon control: Definitions and analysis methods," *Annu. Rev. Control.*, vol. 47, pp. 81–97, 2019.

[9] D. Mahfouz, O. Shehata, and E. Morgan, "Development and evaluation of a unified integrated platoon control system architecture," *IEEE Trans. Intell. Transp. Syst.*, vol. 24, no. 6, p. 5685–5704, 2023.

[10] Z. Ju, H. Zhang, X. Li, X. Chen, J. Han, and M. Yang, "A survey on attack detection and resilience for connected and automated vehicles: From vehicle dynamics and control perspective," *IEEE Trans. Intell. Veh.*, vol. 7, no. 4, pp. 815–837, 2022.

[11] P. Seiler, A. Pant, and K. Hedrick, "Disturbance propagation in vehicle strings," *IEEE Trans. Autom. Control*, vol. 49, no. 10, pp. 35–41, 2004.

[12] S. Xiao, X. Ge, Q.-L. Han, and Y. Zhang, "Dynamic event-triggered platooning control of automated vehicles under random communication topologies and various spacing policies," *IEEE Trans. Cybern.*, vol. 52, no. 11, p. 11477–11490, 2022.

[13] G. Wu, G. Chen, H. Zhang, and C. Huang, "Fully distributed event-triggered vehicular platooning with actuator uncertainties," *IEEE Trans. Veh. Technol.*, vol. 70, no. 7, p. 6601–6612, 2021.

[14] V. Dolk, J. Ploeg, and M. Heemels, "Event-triggered control for string-stable vehicle platooning," *IEEE Trans. Intell. Transp. Syst.*, vol. 18, no. 12, pp. 3486–3500, 2017.

[15] Y. Zhu, H. He, and D. Zhao, "LMI-based synthesis of string-stable controller for cooperative adaptive cruise control," *IEEE Trans. Intell. Transp. Syst.*, vol. 21, no. 11, pp. 4516–4525, 2020.

[16] X. Ge, S. Xiao, Q.-L. Han, X.-M. Zhang, and D. Ding, "Dynamic event-triggered scheduling and platooning control co-design for automated vehicles over vehicular ad-hoc networks," *IEEE/CAA J. Autom. Sin.*, vol. 9, no. 1, pp. 31–46, 2022.

[17] C. Massera, M. Terra, and D. Wolf, "Safe optimization of highway traffic with robust MPC-based cooperative adaptive cruise control," *IEEE Trans. Intell. Transp. Syst.*, vol. 18, no. 11, p. 3193–3203, 2017.

[18] D. G. Nguyen, S. Park, J. Park, D. Kim, J. S. Eo, and K. Han, "An MPC approximation approach for adaptive cruise control with reduced computational complexity and low memory footprint," *IEEE Trans. Intell. Veh.*, pp. 1–13, 2023.

[19] Y. Su, X. Yang, P. Shi, G. Wen, and Z. Xu, "Consensus-based vehicle platoon control under periodic event-triggered strategy," *IEEE Trans. Syst., Man, Cybern.: Syst.*, vol. 54, no. 1, pp. 533–542, 2024.

[20] A. Peters, R. Middleton, and O. Mason, "Leader tracking in homogeneous vehicle platoons with broadcast delays," *Automatica*, vol. 50, no. 1, p. 64–74, 2014.

[21] Y. Zheng, S. Li, J. Wang, D. Cao, and K. Li, "Stability and scalability of homogeneous vehicular platoon: Study on the influence of information flow topologies," *IEEE Trans. Intell. Transp. Syst.*, vol. 17, no. 1, p. 14–26, 2016.

[22] J. Ploeg, N. van de Wouw, and H. Nijmeijer, "$\mathcal{L}_p$ string stability of cascaded systems: Application to vehicle platooning," *IEEE Trans. Control Syst. Technol.*, vol. 22, no. 2, pp. 786–793, 2014.

[23] J. Ploeg, B. Scheepers, E. van Nunen, N. van de Wouw, and H. Nijmeijer, "Design and experimental evaluation of perative adaptive cruise control," in *14th Int. IEEE Conf. Intell. Transp. Syst.*, Washington, DC, USA, 2011, pp. 260–265.

[24] E. van Nunen, J. Reinders, E. Semsar-Kazerooni, and N. van de Wouw, "String stable model predictive cooperative adaptive cruise control for heterogeneous platoons," *IEEE Trans. Intell. Veh.*, vol. 4, no. 2, pp. 186–196, 2019.

[25] A. Samii and N. Bekiaris-Liberis, "Simultaneous compensation of actuation and communication delays for heterogeneous platoons via predictor-feedback CACC with integral action," *IEEE Trans. Intell. Veh.*, pp. 1–13, 2024.

[26] J. Wang, F. Ma, Y. Yang, J. Nie, B. Aksun-Guvenc, and L. Guvenc, "Adaptive event-triggered platoon control under unreliable communication links," *IEEE Trans. Intell. Transp. Syst.*, vol. 23, no. 3, p. 1924–1935, 2022.

[27] X. Guo, J. Wang, F. Liao, and R. Teo, "Distributed adaptive integrated-sliding-mode controller synthesis for string stability of vehicle platoons," *IEEE Trans. Intell. Transp. Syst.*, vol. 17, no. 9, p. 2419–2429, 2016.

[28] F. Gao, S. E. Li, Y. Zheng, and D. Kum, "Robust control of heterogeneous vehicular platoon with uncertain dynamics and communication delay," *IET Intell. Transp. Syst.*, vol. 10, no. 7, pp. 503–513, Sep. 2016.

[29] C. Huang and H. Karimi, "Non-fragile $\mathcal{H}_\infty$ control for LPV-based CACC systems subject to denial-of-service attacks," *IET Control. Theory Appl.*, vol. 15, no. 9, pp. 1246–1256, 2021.

[30] Z. Ju, H. Zhang, and Y. Tan, "Distributed stochastic MPC for heterogeneous vehicle platoons subject to modeling uncertainties," *IEEE Intell. Transp. Syst. Mag.*, vol. 14, no. 2, pp. 25–40, 2022.

[31] B. Wang, Y. Luo, Z. Zhong, and K. Li, "Robust non-fragile fault tolerant control for ensuring the safety of the intended functionality of cooperative adaptive cruise control," *IEEE Trans. Intell. Transp. Syst.*, vol. 23, no. 10, p. 18746–18760, 2022.

[32] Q. Luo, A.-T. Nguyen, J. Fleming, and H. Zhang, "Unknown input observer based approach for distributed tube-based model predictive control of heterogeneous vehicle platoons," *IEEE Trans. Veh. Technol.*, vol. 70, no. 4, pp. 2930–2944, 2021.

[33] S. Wen, G. Guo, B. Chen, and X. Gao, "Cooperative adaptive cruise control of vehicles using a resource-efficient communication mechanism," *IEEE Trans. Intell. Veh.*, vol. 4, no. 1, pp. 127–140, 2019.

[34] Y. Li, W. Chen, S. Peeta, and Y. Wang, "Platoon control of connected multi-vehicle systems under V2X communications: Design and experiments," *IEEE Trans. Intell. Transp. Syst.*, vol. 2, no. 5, p. 891–902, 2020.

[35] D. Swaroop, K. Hedrick, C. Chien, and P. Ioannou, "A comparision of spacing and headway control laws for automatically controlled vehicles," *Veh. Syst. Dyn.*, vol. 23, no. 1, pp. 597–625, 1994.

[36] L. Wang, M. Hu, Y. Bian, G. Guo, S. Li, B. Chen, and Z. Zhong, "Periodic event-triggered fault detection for safe platooning control of intelligent and connected vehicles," *IEEE Trans. Veh. Technol.*, pp. 1–14, 2023.

[37] P. Tabuada, "Event-triggered real-time scheduling of stabilizing control tasks," *IEEE Trans. Autom. Control*, vol. 52, no. 9, pp. 1680–1685, 2007.

[38] Z. Wu, J. Sun, and S. Hong, "RBFNN-based adaptive event-triggered control for heterogeneous vehicle platoon consensus," *IEEE Trans. Intell. Transp. Syst.*, vol. 23, no. 10, p. 18761–18773, 2022.

[39] H. Li, Z. Chen, B. Fu, Z. Wu, X. Ji, and M. Sun, "Event-triggered vehicle platoon control under random communication noises," *IEEE Access*, vol. 9, pp. 51 722–51 733, 2021.

[40] Y. Wei, W. Liyuan, and G. Ge, "Event-triggered platoon control of vehicles with time-varying delay and probabilistic faults," *Mech. Syst. Signal Process.*, vol. 87, pp. 96–117, 2017.

[41] A. Girard, "Dynamic triggering mechanisms for event-triggered control," *IEEE Trans. Autom. Control*, vol. 60, no. 7, pp. 1992–1997, 2015.

[42] H. Zhang, J. Liu, Z. Wang, H. Yan, and C. Zhang, "Distributed adaptive event-triggered control and stability analysis for vehicular platoon," *IEEE Trans. Intell. Transp. Syst.*, vol. 22, p. 1627–1638, 2021.

[43] D. Borgers and M. Heemels, "Event-separation properties of event-triggered control systems," *IEEE Trans. Autom. Control*, vol. 59, no. 10, pp. 2644–2656, 2014.

[44] A. Selivanov and E. Fridman, "Event-triggered $\mathcal{H}_\infty$ control: A switching approach," *IEEE Trans. Autom. Control*, vol. 61, no. 10, pp. 3221–3226, 2016.

[45] K. Gu, V. Kharitonov, and J. Chen, *Stability of Time-Delay Systems*. Birkhäuser Boston, 2003.

[46] L. Mozelli, R. Palhares, and G. Avellar, "A systematic approach to improve multiple Lyapunov function stability and stabilization conditions for fuzzy systems," *Inf. Sci.*, vol. 179, no. 8, pp. 1149–1162, 2009.

[47] S. Boyd, L. El Ghaoui, E. Feron, and V. Balakrishnan, *Linear Matrix Inequalities in System and Control Theory*. Philadelphia, PA: SIAM, 1994, vol. 15.

[48] R. Rajamani, *Vehicle Dynamics and Control*. Boston, MA: Springer US, 2012.

[49] K. Khalil, *Nonlinear Systems*, 3rd, Ed. Prentice Hall, 2002.

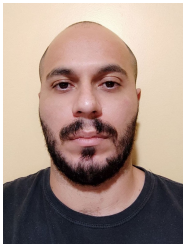

Rafael N. Silva received his B.Sc. degree in Electrical Engineering from Instituto Federal da Bahia, Brazil, in 2017, and the M.Sc. degree in Electrical Engineering from Universidade Federal de Minas Gerais, Brazil, in 2020. He is currently pursuing a joint Ph.D. degree at Universidade Federal de Minas Gerais, Brazil, and Université Polytechnique Hauts-de-France, Valenciennes, France. His research interests include linear systems and control theory.

Anh-Tu Nguyen (M'18, SM'21) is an Associate Professor at the INSA Hauts-de-France, Université Polytechnique Hauts-de-France, Valenciennes, France. He received the degree in engineering and the M.Sc. degree in automatic control from Grenoble Institute of Technology, France, in 2009, and the Ph.D. degree in automatic control from the University of Valenciennes, France, in 2013. He is an Associate Editor for several journals such as IEEE/ASME TMECH, IEEE T-ITS, IFAC CEP, ISA Transactions. His research interests include robust control and estimation, human-in-the-loop control, and mechatronic applications.

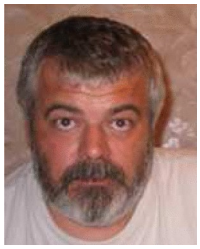

Thierry-Marie Guerra received the Ph.D. degree in automatic control in 1991 from University of Valenciennes, France, in 1999. He is a Full Professor with the Polytechnic University Hauts-de-France, France. His research fields are Takagi-Sugeno control and observation, LMI constraints and applications to mobility, soft robotics, and disabled persons. Prof. Guerra is a chair of the IFAC Technical Committee 3.2 "Computational Intelligence in Control", an Associate Editor of FSS and IEEE TFS.

Fernando O. Souza obtained his B.S. (2003) degree in Control and Automation Engineering from the Pontifícia Univ. Católica de Minas Gerais, Brazil, and his M.S. (2005) and Ph.D. (2008) degrees in Electrical Engineering from the Univ. Fed. de Minas Gerais (UFMG), Brazil. He is currently a Professor at the Department of Electronic Engineering, UFMG. His research interests include multi-agent systems, time delay systems, and robust control.

Luciano Frezzatto received his B.Sc. degree in Computer Engineering, M.Sc. degree in Mechanical Engineering and Ph.D. degree in Electrical Engineering from University of Campinas, Brazil, in 2009, 2011 and 2017, respectively. From 2015 to 2016, he did an internship at University of California, San Diego, USA. He is a Professor at the Department of Electronics Engineering, Universidade Federal de Minas Gerais, Brazil. His research interests include fuzzy/LPV control theory and applications.